Physics and Chemistry of the Earth 132 (2023) 103452

Contents lists available at ScienceDirect

Physics and Chemistry of the Earth

journal homepage: www.elsevier.com/locate/pce

Have COVID lockdowns really improved global air quality? –Hierarchical observations from the perspective of urban agglomerations using atmospheric reanalysis data

Rahul Deb Das [a], Subhajit Bandopadhyay [b,*], Subhasis Ghosh [c,**], Mridul Das [d], Mousumi Chowdhury [e], Alexander Cotrina-Sanchez [f], Chandan Kumar [g,h], Chandana Mitra [c]

[a] IBM, Munich, Germany
[b] School of Geography and Environmental Science, University of Southampton, Southampton, SO17 1BJ, UK
[c] Department of Geosciences, Auburn University, Auburn, Alabama, USA
[d] Department of Geography, Serampore College, West Bengal, India
[e] Department of Mining Engineering, Indian Institute of Engineering Science & Technology, Shibpur, India
[f] Department for Innovation in Biological, Agri-Food and Forest Systems, Università Degli Studi Della Tuscia, Via San Camillo de Lellis, Snc, 01100 Viterbo, Italy
[g] Department of Plant and Soil Sciences, Mississippi State University, 75 B. S. Hood Rd, Mississippi State, MS 39762, USA
[h] Crop Production Systems Research Unit, United States Department of Agriculture -Agricultural Research Service, Stoneville, Mississippi, USA

ARTICLE INFO

Keywords:
COVID lockdown
Air quality
Meso-regional
Remote sensing
Urban agglomeration

ABSTRACT

COVID-19 cases surged in late 2019, leading to worldwide lockdowns that closed non-essential places and activities, industries, and businesses to halt the spread of the virus. Many studies suggested improved air quality during lockdowns. However, these findings often focused on core city limits and did not account for heavy pollution sources outside cities (around the fringe areas), such as factories, power plants, and coal mines, which operated continuously for energy needs even during lockdowns. Therefore, this study quantified and re-analyzed the air quality data using a top-down approach. This study analyzed six major air quality parameters namely SO_2, O_3, NO_2, $PM_{2.5}$, AOD_{500}, and UAI. The time-averaged approach was adopted to analyze the data followed by ground validation. High variability and anomalies in air quality parameters were observed at different levels of observations (i.e. city level, country level, etc.). However, it was found that during the lockdown period, $PM_{2.5}$ and NO_2 significantly dropped at the country level with few exceptions. Changes were also observed in AOD_{500}, O_3, and UAI concentrations from city to country scale. Mixed behaviors among the atmospheric pollutants were observed with changes in scale and time. This makes the claim about air quality improvements during COVID-19 lockdowns very relative to the scale of observation and the pollutant indicators being referred to. Multi-layered analyses of pollutant concentrations extending beyond the city limits to the meso-regional levels with varying space-time observations made the present work unique from existing literature that claimed a global air quality improvement during the COVID-19 lockdown period.

1. Introduction

The emergence and development of the COVID-19 pandemic has pushed the world civilizations towards a 'new normal' over the years. While many countries are still struggling to end this chapter of crisis, a new concern is being put forward by the scientific community regarding the contribution of past COVID-19 lockdowns on air quality improvements (Ravindra et al., 2022). The fast-spreading nature of this virus forced governments to impose large-scale restrictions on outdoor human mobility and activities to protect public health (Kharroubi and Saleh, 2020). These strict restrictions (also known as lockdowns or stay-at-home orders) forced people to stay home, shutting down all non-essential public places, industrial activities, and businesses to slow down the transmission of the virus (Spiegel and Tookes, 2022). Some researchers claimed that due to such restrictions, major human activities were impaired over a significant time leading to improved air quality

* Corresponding author.
** Corresponding author.
E-mail addresses: subhajit.iirs@gmail.com (S. Bandopadhyay), subhasis@auburn.edu (S. Ghosh).

https://doi.org/10.1016/j.pce.2023.103452
Received 27 February 2023; Received in revised form 24 July 2023; Accepted 26 July 2023
Available online 3 August 2023

Table 1
List of different studies that claimed improved air quality during COVID-19 lockdowns (as to the knowledge of the authors). The table also shows the study periods, implemented methods, and important findings.

Study	Location	Type of study/method	Period	Findings/Remarks
Aman et al. (2020)	Ahmedabad, India	Air quality monitoring using remote sensing data	2015–2020	Decrease in Suspended Particulate Matter
Adam et al. (2021)	USA (cities from all states)	Air quality monitoring using station data	Beginning weeks in 2020	$PM_{2.5}$: +3.0 O_3: -4.0 NO_2: -30.0
Abdullah et al. (2020)	Malaysia (over 16 states)	Air quality monitoring using station data	14–17 March 2020	$PM_{2.5}$: -42.6 to -76.5
Barré et al. (2021)	100 European cities	Satellite data (TROPOMI), air quality monitoring station data, air quality model simulations	February–April 2019	NO_2: +6.05% to -60.5%
Chen et al. (2020)	China (367 cities)	Satellite observation (Sentinel-5)	5th January – January 20, 2020 compared to the same period in 2019	NO_2: -12.9 μg/m^3, $PM_{2.5}$: -18.9 μg/m^3
Dantas et al. (2020)	Brazil (Rio de Janeiro; district-wise study)	monitoring station data	March–April 2018, 2019, 2020	PM_{10}: +28.7 to1+9.4, NO_2: -24.1 to -32.9 CO: -37.0 to -43.6 O_3: +22.5 to +63
Gautam (2020)	India (city-based study)	Multi-sourced satellite-based observations	March April 2016–2020	About 50% improvement in air quality
Addas and Maghrabi (2021)	World (237 papers)	Literature Review	Pre-lockdown and Post-lockdown period	Significant improvement in air quality all over the world
Rana et al. (2021)	China	Literature Review	Before and after the lockdown	Improvement of air quality with spatial variation
Duc et al. (2021)	Australia (Sydney region)	Satellite observation and station data monitoring	Pre and Post lockdown (April–June 2020)	A small reduction in atmospheric pollutant concentrations
Angom et al. (2021)	East Africa (Kampala, Nairobi, and Dar es Salaam cities of Uganda, Kenya and Tanzania)	Multi-sourced satellite observations	Comparison between Pre and post-lockdown periods	Air quality improved during the lockdown; started to deteriorate once the restrictions were lifted
Kutralam-Muniasamy et al. (2021)	Mexico City	Multi-sourced satellite observations	Comparison between lockdown and pre-lockdown period	Improvements in air quality parameters
Schiavo et al. (2022)	Monterrey city, Mexico	Multi-sourced satellite observations	Comparison among pre-lockdown, lockdown, and unlock period	Major improvement in Air Quality Index; Found an association between air pollutants and economic activity and suggests that it can be used in future strategies to improve urban air quality.
Behera et al. (2022)	India	Multi-sourced satellite observations	Pre lockdown Vs post lock down comparison based on NO_2, SO_2, HCHO, CH_4, CO, UVAI, O_3	Improvements in air quality during COVID-19 lockdowns

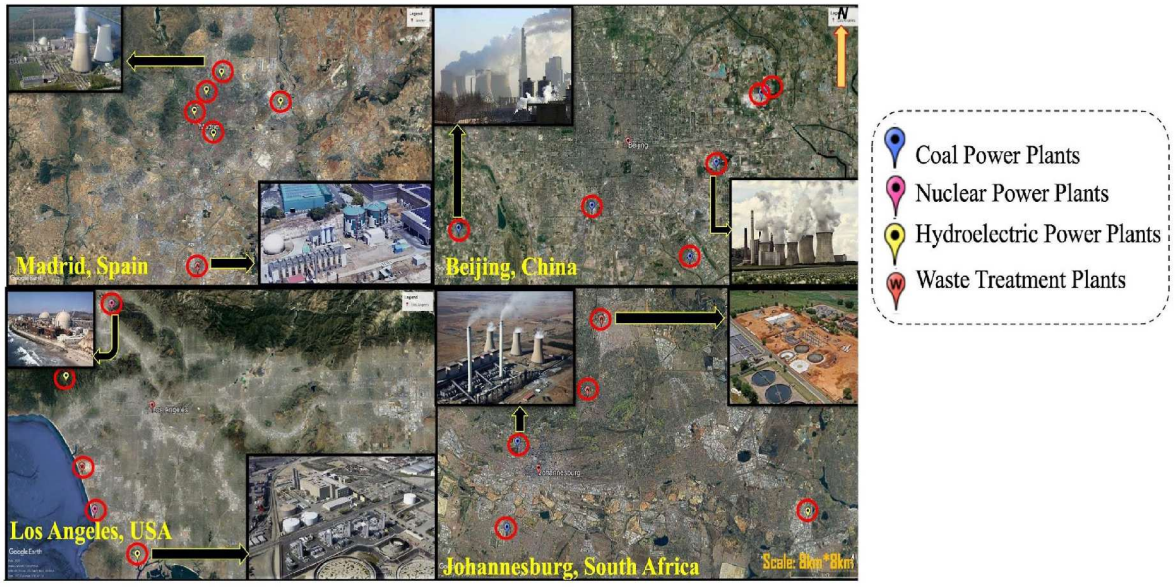

Fig. 1. Presence of 24 × 7 industrial and power plants and wastewater treatment plants located at the urban agglomerated zones of selected cities. Source: Google Earth.

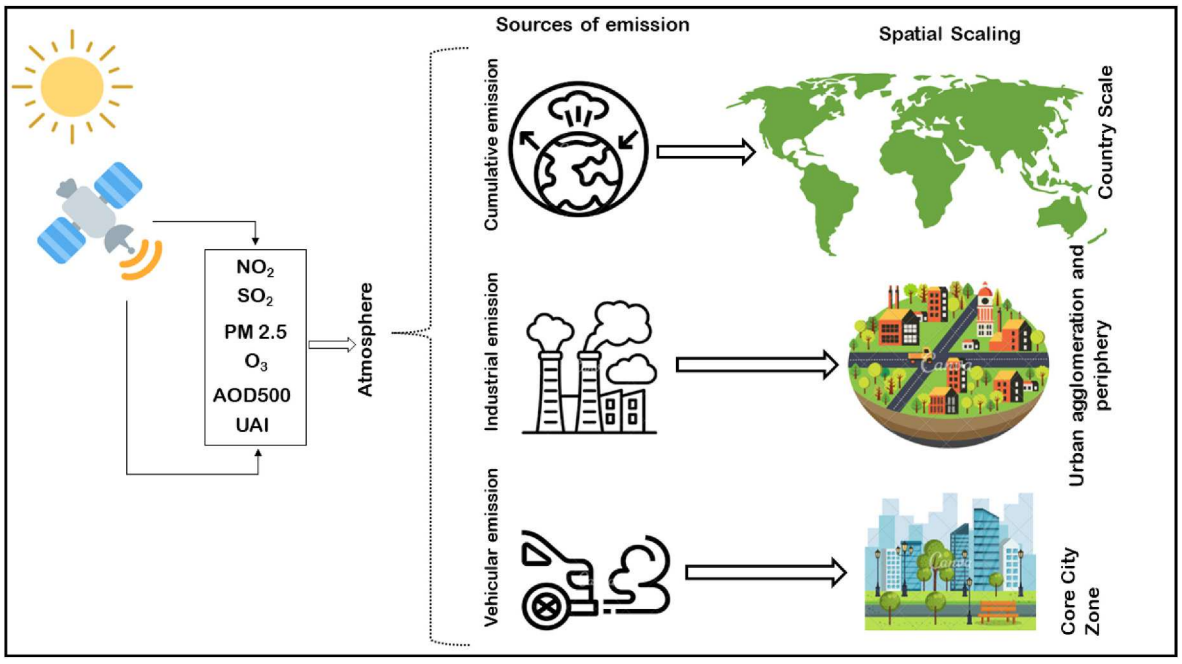

Fig. 2. Conceptual framework showing sources of emissions at different scales.

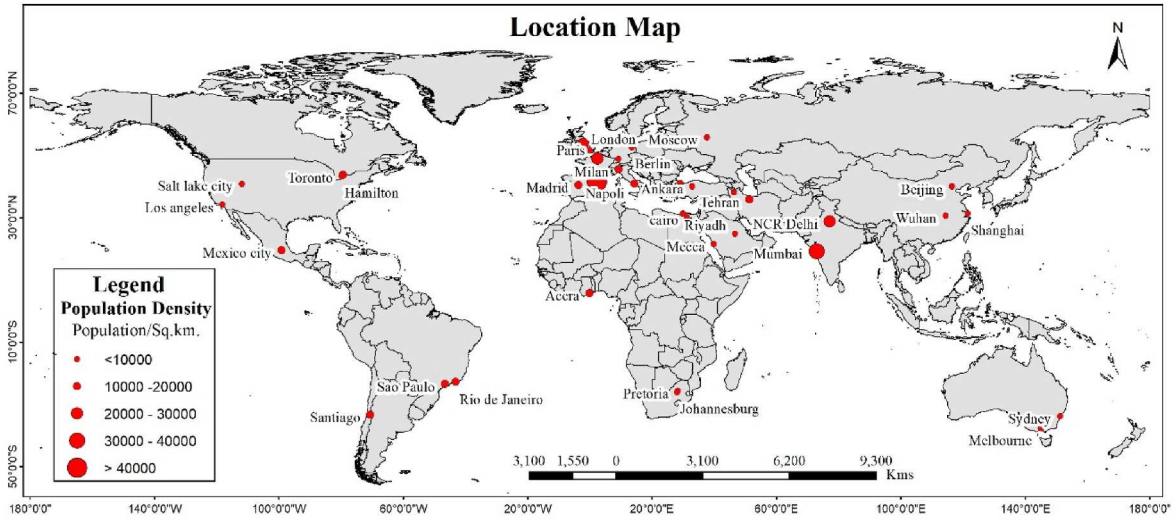

Fig. 3. Location of the global cities studied in this research. Red dots represent the population density of the cities.

across the world (Agarwal et al., 2021; Gautam, 2020; Jephcote et al., 2021; Menut et al., 2020; Rodríguez-Urrego & Rodríguez-Urrego, 2020). Air pollution has become a major matter of concern for mankind in past few decades (Manisalidis et al., 2020). In the course of time, due to heavy industrialization and increased vehicular use, a constant deterioration of global air quality has been observed (Chen and Kan, 2008; Molina and Molina, 2004) intensifying global warming and adversely affecting human health. The primary pollutants responsible for degrading air quality are Nitrogen Oxides (NO_2), Carbon monoxide (CO), Sulfur dioxide (SO_2), Ozone (O_3), particulate matters (PM) of varying sizes (e.g., $PM_{2.5}$ and PM_{10}), and various volatile organic compounds (VOC) or hydrocarbons. The majority of these pollutants are added to the atmosphere by various anthropogenic activities like burning fossil fuel, emissions from motor vehicles, burning of tires, and industrial and factory waste (Popescu and Ionel, 2010). However, during the COVID-19 pandemic lockdowns, emissions from human activities were stalled and improvements in air quality in many cities have been reported (Table 1). These studies monitoring the lockdown period reported a significant decrease in transportation and industrial activities causing a drop in air pollution indicators in many places around the world (Gardiner, 2020). Citing the results, such case studies claimed that air quality in general had significantly improved during the COVID-19 lockdown period.

However, it should be noted that all these studies were focused on -

1. Geographical areas with a dense population (i.e. mega cities)
2. Places having the highest accessibility to public operations for goods and services
3. Economic zones where industrial, residential, commercial, and administrative activities are carried out.

Table 2
Details of sample countries and cities (based on the total number of infected COVID-19 cases and pollution index).

Country	City
USA	Los Angeles
USA	Salt Lake City
Brazil	Sao Paulo
Brazil	Rio De Janeiro
France	Paris
France	Marseille
Turkey	Istanbul
Turkey	Ankara
Spain	Barcelona
Spain	Madrid
Australia	Sydney
Australia	Melbourne
Germany	Stuttgart
Germany	Berlin
China	Beijing
China	Shanghai
China	Wuhan
UK	London
UK	Manchester
Mexico	Mexico City
Saudi Arabia	Mecca
Saudi Arabia	Riyadh
South Africa	Pretoria
South Africa	Johannesburg
Ghana	Accra
Russia	Moscow
India	Mumbai
India	NCR Delhi
Italy	Milan
Italy	Napoli
Iran	Tabriz
Iran	Tehran
Egypt	Alexandria
Egypt	Cairo
Chile	Santiago
Canada	Hamilton
Canada	Toronto

During the lockdown periods, anthropogenic activities were temporarily restricted in these areas. This restriction might have improved air quality within city limits, as reported by studies (Table 1). However, these studies may not have fully reflected the overall air pollution levels beyond the city's core boundaries, where major polluting hotspots like factories, power plants, and coal mines are located (Burke et al., 2019). These polluting hotspots are generally located outside the proximity of the core city due to environmental norms and public safety issues. However, they often contribute to the main city's pollution levels depending on meteorological factors like wind speed, wind direction etc, and largely contribute to regional and global pollution levels (Fig. 1).

Power plants, coal mines, and similar facilities are considered essential services due to their role in ensuring a country's energy security. As a result, they operated continuously even during the lockdown period. Because the existing studies did not adequately consider the contributions from these areas, the authors suggest a re-analysis of the situation from an urban agglomeration or urban archipelagos perspective (Shepherd et al., 2013). This approach would provide a better understanding of the claims regarding air quality improvements during COVID-19 lockdowns. In simple terms, urban agglomerations are large clusters of urban spaces where smaller towns have either merged or are in the process of merging with a larger adjacent city due to inter-related socio-economic activities (Fang and Yu, 2017). Hence, this encompasses a larger geographical extent, collectively impacting the surrounding environment in the vicinity. In this case, considering urban agglomerations gave us an opportunity to include the emissions of out-of-the-city power plants, coal mines etc along with city emissions, helping to perform a robust analysis of a much bigger area. This paper systematically presents this new perspective that investigates the change in major air quality parameters at different granularity to understand how air quality responded during the COVID-19 lockdown period with space-time variations (Fig. 2).

Periodic observations conducted from globally gridded atmospheric reanalysis products (i.e. OMI, MERRA-2, TOMS etc.) developed from the assimilation of earth observation satellites.

Table 3
Properties of major air pollutants.

Pollutant	Source	End Product	Occurrence	Avg. Lifetime (approx.)
Nitrogen oxides (e.g., NO)	Fossil fuel combustion (Tian et al., 2020)	NO_2, HNO_3	Urban environments under stable atmospheric conditions	1–12 h (Lorente et al., 2019)
Hydrocarbons	Fossil fuel combustion, solvent, evaporation, vegetation (Ravindra et al., 2008)	Oxygenated organic compounds	Urban environment	40 days (Gaur et al., 2022)
Carbon monoxide (CO)	Incomplete fossil fuel combustion (Badr and Probert, 1994)	CO_2	Urban environment, industrial areas	2 months (Khalil and Rasmussen, 1990)
Ozone (O_3)	Hydrocarbons, nitrogen oxides, and sunlight (Wang et al., 2022)	Smog	Suburban and rural areas	23 days (The Royal Society, 2008)
Sulfur dioxide (SO_2)	Fossil fuel combustion, industrial emission (Smith et al., 2011)	H_2SO_4	Urban environment, industrial and mining areas	13 h–48 h (Junkermann and Roedel, 1983)
Particulate Matter (PM)	Combustion wear and tear, abrasion, dust (Mukherjee and Agrawal, 2017)	–	Urban, industrial, and mining area	10–100 h (Esmen and Corn, 1971)

Table 4
Parameters and data sources.

Air Quality Parameter	Unit	Data Source	Spatial Resolution	Temporal Resolution
Nitrogen dioxide (NO_2)	molecules/cm^2	Ozone Monitoring Instrument (OMI) (Kleipool et al., 2022)	0.25°	Daily
Sulfur dioxide (SO_2)	kg/m^3	Modern-Era Retrospective Model (MERRA-2) (Global Modeling and Assimilation Office, 2015)	0.5°	Hourly
Particulate Matter ($PM_{2.5}$)	kg/m^3	Modern-Era Retrospective Model (MERRA-2) (Global Modeling and Assimilation Office, 2015)	0.5°	Hourly
Ozone (O_3)	DU	Meteor-3 Total Ozone Mapping Spectrometer (TOMS) (TOMS Science Team, 1996)	1.0° * 1.25°	Daily
Aerosol Optical Depth 500nm (AOD_{500})	–	Ozone Monitoring Instrument (OMI) (TOMS Science Team, 1996)	1.0°	Daily
Ultra-Violet Aerosol index (UAI)	–	Ozone Monitoring Instrument (OMI) (TOMS Science Team, 1996)	1.0°	Daily

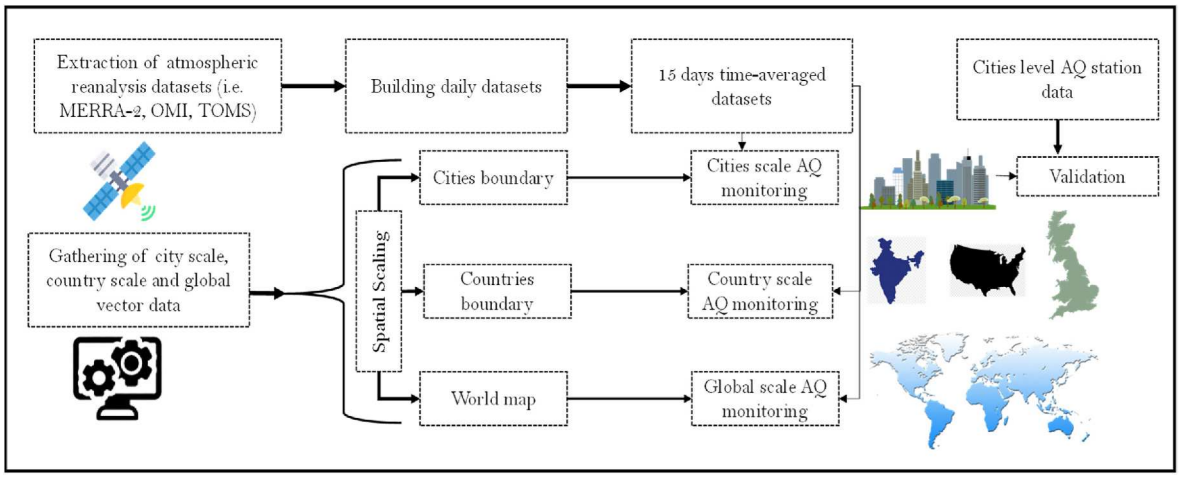

Fig. 4. Methodological framework of the workflow adopted by this study. AQ denotes air quality.

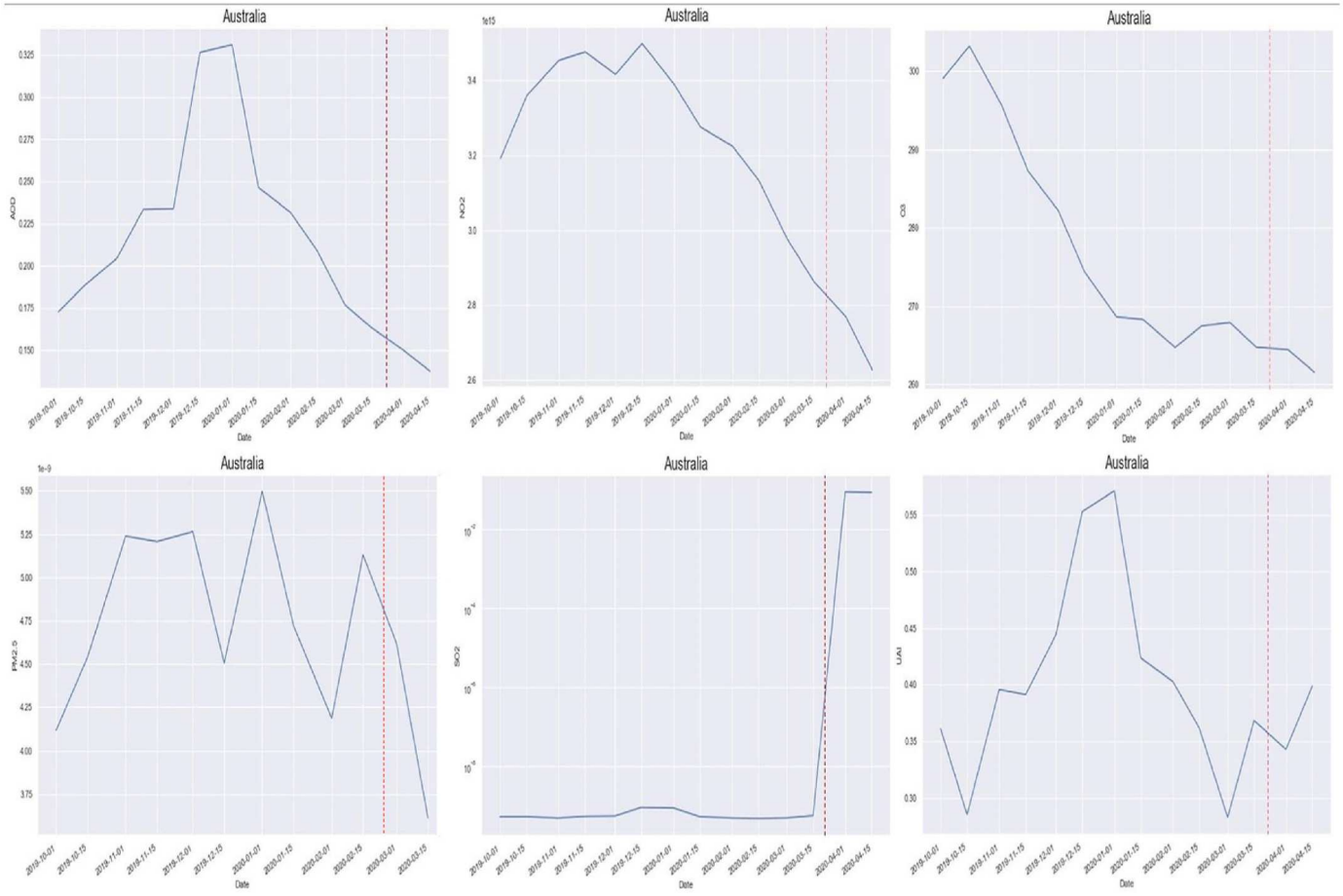

Fig. 5. Temporal change of six air quality parameters in Australia. The red vertical line indicates the lockdown date.

The study considers and observes the changes in major air quality parameters such as SO_2, O_3, NO_2, $PM_{2.5}$, aerosol optical depth (AOD) at 500 nm, and UV Aerosol index (UAI). We believe this research will help validate the claims regarding improved air quality induced by COVID-19 lockdowns from a multi-scaled hierarchical viewpoint that is limited in the available literature. Sections 2 of this article present the research questions; section 3 describes the methodology and datasets used for the analyses; section 4 presents the results followed by a brief discussion and conclusion in section 5 and 6. The present research seeks to answer the following research questions.

- How did COVID-19 lockdown impact regional and global air quality at different levels?
- How effectively can the change in air quality be monitored using spaceborne remote sensing systems?

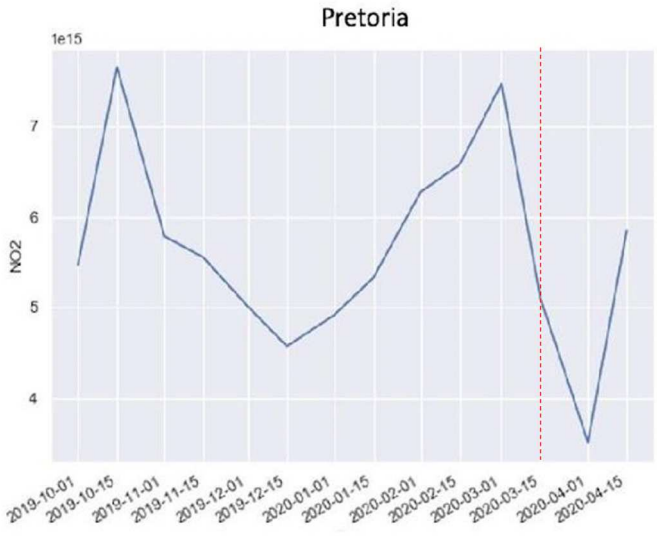

Fig. 6. Temporal change of NO_2 over Pretoria, South Africa (Units are in molecules per cm^2).

2. Methodological framework

To understand the temporal trend of air quality parameters, changes in five major atmospheric variables e.g. three major pollutant gases (i.e. NO_2, SO_2, O_3), and aerosols in terms of AOD 160 at 500 nm and UV Aerosol index along with $PM_{2.5}$ were observed over 20 countries and 37 selected cities (Fig. 3, Table 2) using multiple spaceborne observation techniques.

The detailed information of these spaceborne observations along with their spatial and temporal resolutions are on Table 3. The selection of countries and their cities are entirely based on three parameters: (1) geographical size of the country, (2) number of COVID cases, and (3) pollution index. The list of the countries and their number of COVID cases were obtained from WHO Coronavirus (COVID-19) Dashboard (https://covid19.who.int/) whereas the pollution index of that particular county was obtained from IQ Air quality ranking (https://www.iqair.com/world-air-quality-ranking).

While delineating the city boundaries, special attention was given towards the incorporation of any power plant, coal mine, water treatment plant, etc that were present beyond the city's administrative boundaries since they also contribute largely to emitting pollutants. Google Earth was referred for the detection of these sites (Fig. 1). Cloud computing techniques were used to collect and process the required datasets from NASA Giovanni (https://giovanni.gsfc.nasa.gov/giovanni/) and Google Earth Engine (https://earthengine.google.com/). A global comparative analysis of pre-lockdown, during-lockdown, and post-lockdown conditions was performed following a top-down approach. In spatial analysis, the top-down approach refers to a methodological perspective that starts with a broad-scale analysis and gradually zooms in to examine finer details. This approach involves analyzing and understanding spatial patterns and processes at larger scales before focusing on smaller spatial units or individual objects. The top-down approach is often used to gain a holistic understanding of spatial phenomena and to identify general patterns or trends before

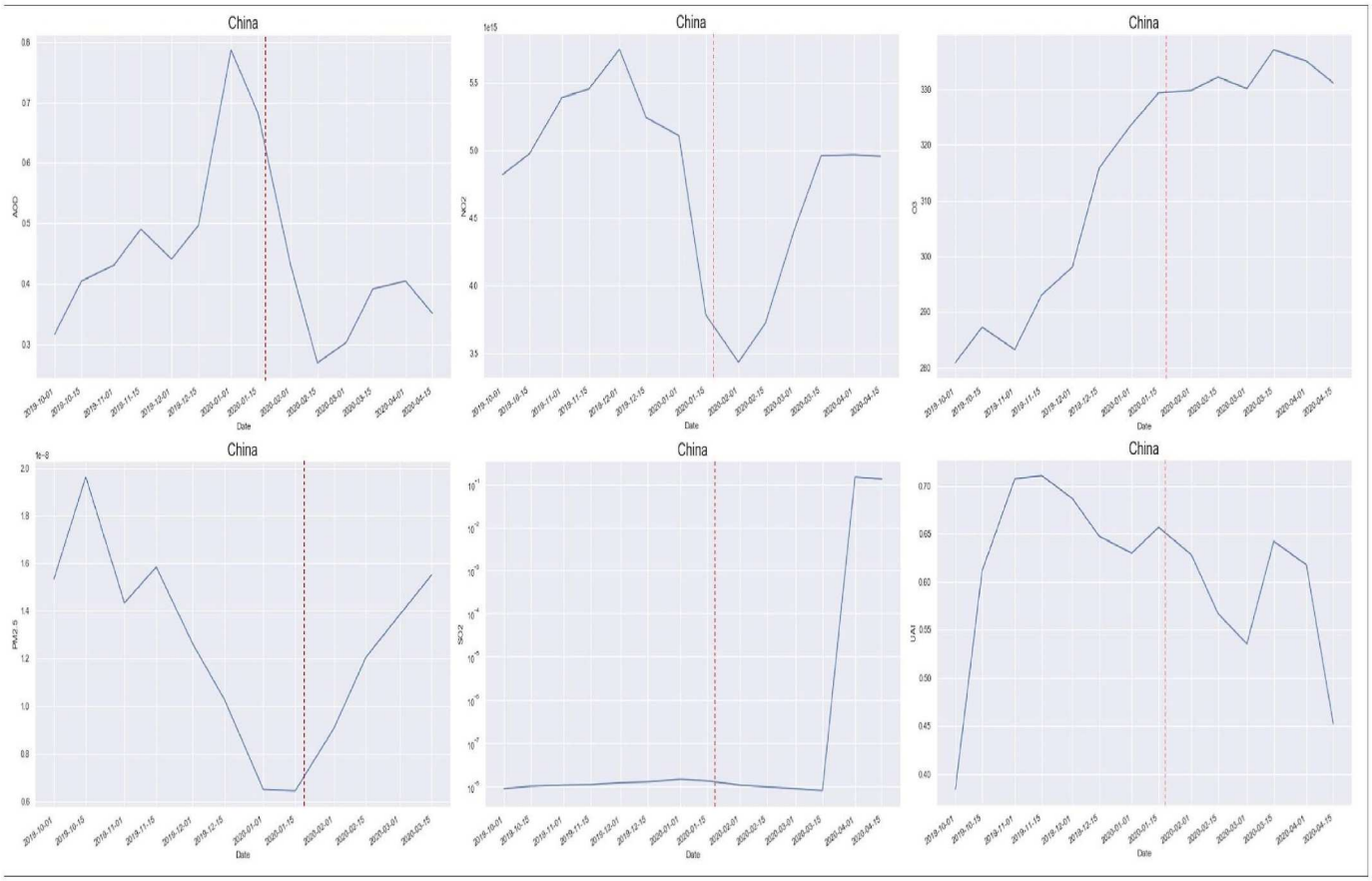

Fig. 7. Temporal change of six air quality parameters in China. The red vertical line indicates the lockdown date.

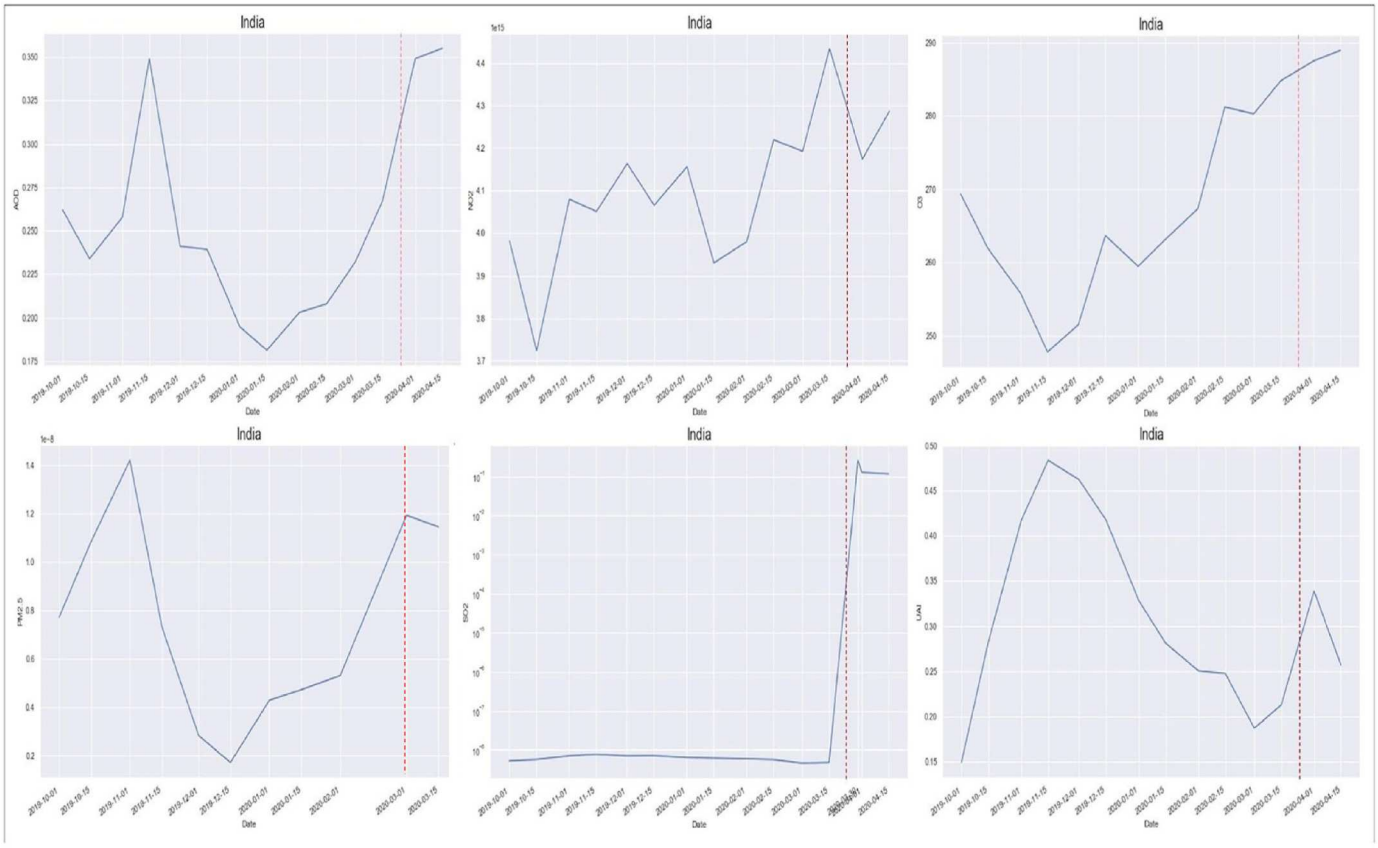

Fig. 8. Temporal change of six air quality parameters in India. The red vertical line indicates the lockdown date.

delving into specific details (Eicken et al., 2021).

2.1. Dataset

To understand the temporal trend of air quality parameters (NO_2, SO_2, $PM_{2.5}$, O_3, AOD_{500}, UAI) of 37 cities in 20 countries (Table 2), this study used multiple spaceborne remote sensing observations. The detailed information of these spaceborne observations along with their spatial and temporal resolutions are on Table 4.

Ozone Monitoring Instrument (OMI) was used to observe NO_2, AOD_{500}, and UAI level. OMI is a visual and ultraviolet spectrometer aboard NASA's Aura spacecraft (Ahmad et al., 2003). The Ozone Monitoring Instrument (OMI) utilizes a hyperspectral imaging push-broom system with 740 bands to observe the backscatter signal from the Earth's surface in the visible and ultraviolet spectrum. While it provides a high spectral resolution, the spatial resolution is relatively low at 13 km × 24 km, with the possibility of zooming or resampling for higher spatial resolution (Levelt et al., 2006). However, the OMI's hyperspectral and high temporal capability makes it suitable for observing urban pollution on a broader scale (Levelt et al., 2018).

In order to measure O_3, Meteor-3 Total Ozone Mapping spectrometer (TOMS) was used. Meteor-3 has been developed and launched by NASA on board Earth Probe Satellite (TOMS-EP) providing long-term daily mapping of the global distribution of the earth's atmospheric ozone. In this research, the authors used TOMS Level-3 data which contains daily total ozone and reflectivity at 1° latitude by 1.25° longitude spatial grid. To measure SO_2 and $PM_{2.5}$ concentration, Modern-Era Retrospective analysis for Research and Applications, Version 2 (MERRA-2) observation was used. MERRA-2 is the latest atmospheric reanalysis of the modern satellite era produced by NASA's Global Modeling and Assimilation Office (GMAO). MERRA-2 provides a long-term record of global atmospheric analyses with a regular grid, homogeneous record of the global atmosphere. It provides additional aspects of the climate system including trace gas constituents. MERRA-2 provides information at a low spatial resolution of 0.5° (approx. 50 km) along the latitudinal direction (Ding et al., 2021).

2.2. Method of analysis

This study investigated the changes in air quality parameters under observation during lockdown months in 2020 compared to the same time frame in 2019 (October 2019–April 2020). It measured the concentrations of the air quality parameters and did a comparative analysis between the before-lockdown and after-lockdown scenarios. In contrast to the state-of-the-art technique that is mostly focused on the city level, the study used a top-down approach to understand the responses of the air quality parameters during pre and post-lockdown situations at a varying spatial scale that starts from the city level and gradually goes up to the country level. Once the data sets were selected, they were processed in the NASA Giovanni open web environment (Acker and Leptoukh, 2007). For each parameter, a raster containing the satellite observations of the given air quality parameter was selected from the NASA Giovanni platform. Each raster contains the value of the given air quality parameter at each grid averaged over the past 15 days. This

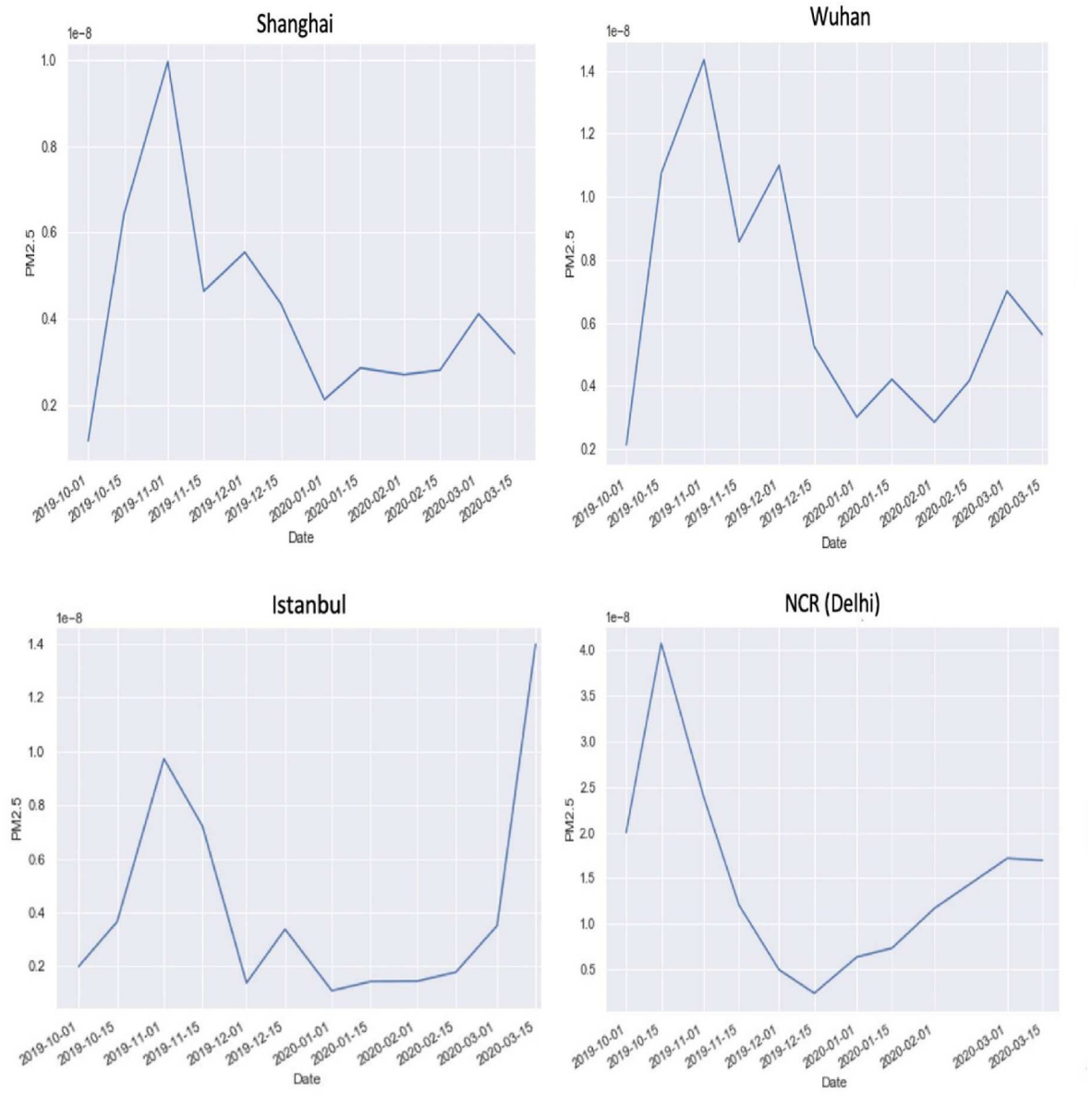

Fig. 9. Temporal change of $PM_{2.5}$ over Shanghai, Wuhan, Istanbul, Delhi NCR (Units are in kg/m3).

process is continued from October 1, 2019 to 30th April 2020. Then for each country-level raster, the mean was calculated over the entire image to study the trend at an interval of 15 days. The reason behind the selection of 15 days intervals is due to the unavailability of daily or weekly products from the NASA Giovanni archive. To investigate at a city level, each country raster was clipped using the city and urban archipelago shape files, and then mean values were calculated. During the city-level processing, data gaps were observed mostly for SO_2 and AOD_{500} parameters that have been filled with the nearest pixel values through interpolation (Feizizadeh & Blaschke, 2013). The overall process workflow is shown in Fig. 4. The investigation was broken down into three phases. In the first phase, trends of air quality parameters were measured for a continuous time period (i.e. October 1, 2019 to April 30, 2020) for both city and country scales; In the second phase, the same parameters were compared between the months of March–April 2019 and March–April 2020 for all sample countries and the sample cities; and in the last phase, city-level pollutant parameters of first and last 15 days of April 2020 were compared. Satellite-based measurements were further validated in reference to ground-based air quality measurement data published by IQAir. However, due to the unavailability of all studied parameters (i.e. SO_2, O_3, NO_2, $PM_{2.5}$, AOD_{500}, UAI) in the IQAir portal, ground validation was performed for $PM_{2.5}$ only.

3. Results

3.1. Phase I: city to country level relative observations of the air quality parameters for the continuous timeframe- October 1, 2019 to April 30, 2020

In this phase, the trend in air quality parameters at both the city level

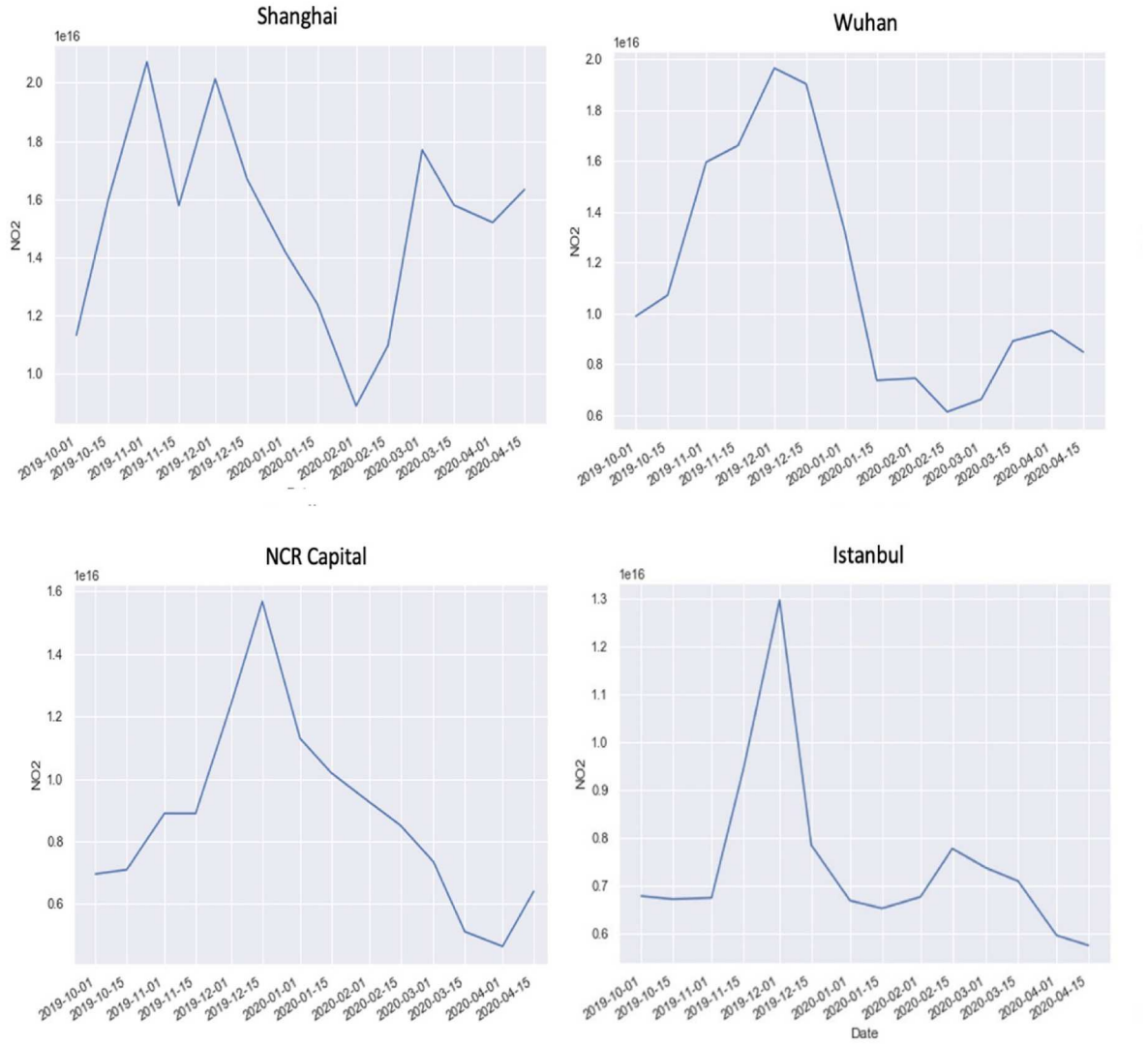

Fig. 10. Temporal change of NO_2 in Shanghai, Wuhan, Delhi NCR, Istanbul (Units are in molecules per cm^2).

and country level over a continuous time period (from October 1, 2019 to April 30, 2020) has been analyzed.

3.1.1. Australia and oceania

Based on the analysis the Oceania region and Australia showed a mixed pattern for UAI and a gradual declining pattern for NO_2, O_3, $PM_{2.5}$, AOD_{500} (Fig. 5). The country-wide lockdown was initiated from around March 23, 2020. From October 2019, NO_2 showed an increasing pattern till December 15, 2020 and reached above 3.4 molecules per cm^2. The UAI profile of Australia as a country shows an increasing pattern with the highest peak at 0.55 on January 1, 2020 followed by a decline below 0.30 on March 1, 2020. It was observed that in Sydney, Australia, the $PM_{2.5}$ level was less than 1 $\mu g/m^3$ except for the month of January 2020 when the $PM_{2.5}$ level reached approximately 2.45 $\mu g/m^3$. On the other hand, Melbourne, Australia showed an overall mixed pattern with $PM_{2.5}$ ranging from 0.73 $\mu g/m3$ to 2.45 $\mu g/m^3$ with two prominent peaks on November 1, 2019–November 30, 2019 and January 15, 2020–January 31, 2020.

3.1.2. Africa

In Pretoria, the NO_2 profile showed a mixed pattern ranging from 4.5 molecules per cm^2 to 7.0 molecules per cm^2 with a peak above 7.0 molecules per cm^2 (Fig. 6). South Africa overall showed a mixed trend for $PM_{2.5}$, SO_2, and UAI, whereas a drop in AOD_{500}, NO_2, and O_3 from March 15, 2020 which is 11 days before the lockdown was imposed there.

3.1.3. Asia

In Asia, China showed a drop in $PM_{2.5}$ from November 15, 2019 to January 31, 2020. Similar (short-term) declining trend can be seen for AOD_{500} and NO_2 from January 1, 2020 to February 29, 2020, whereas SO_2 shows an increasing pattern after March 15, 2020 (Fig. 7).

In terms of $PM_{2.5}$, Shanghai and Wuhan show a declining trend from November 1, 2019 (Fig. 9) while UAI shows a mixed pattern ranging between 0.50 and 0.65. The NO2 profile of Wuhan shows a mixed pattern, reaching up to 0.6 molecules per cm^2 on January 1, 2020 followed by a sudden drop thereafter. This can be justified as the major travel restriction was imposed on 23rd January in Wuhan which reduced

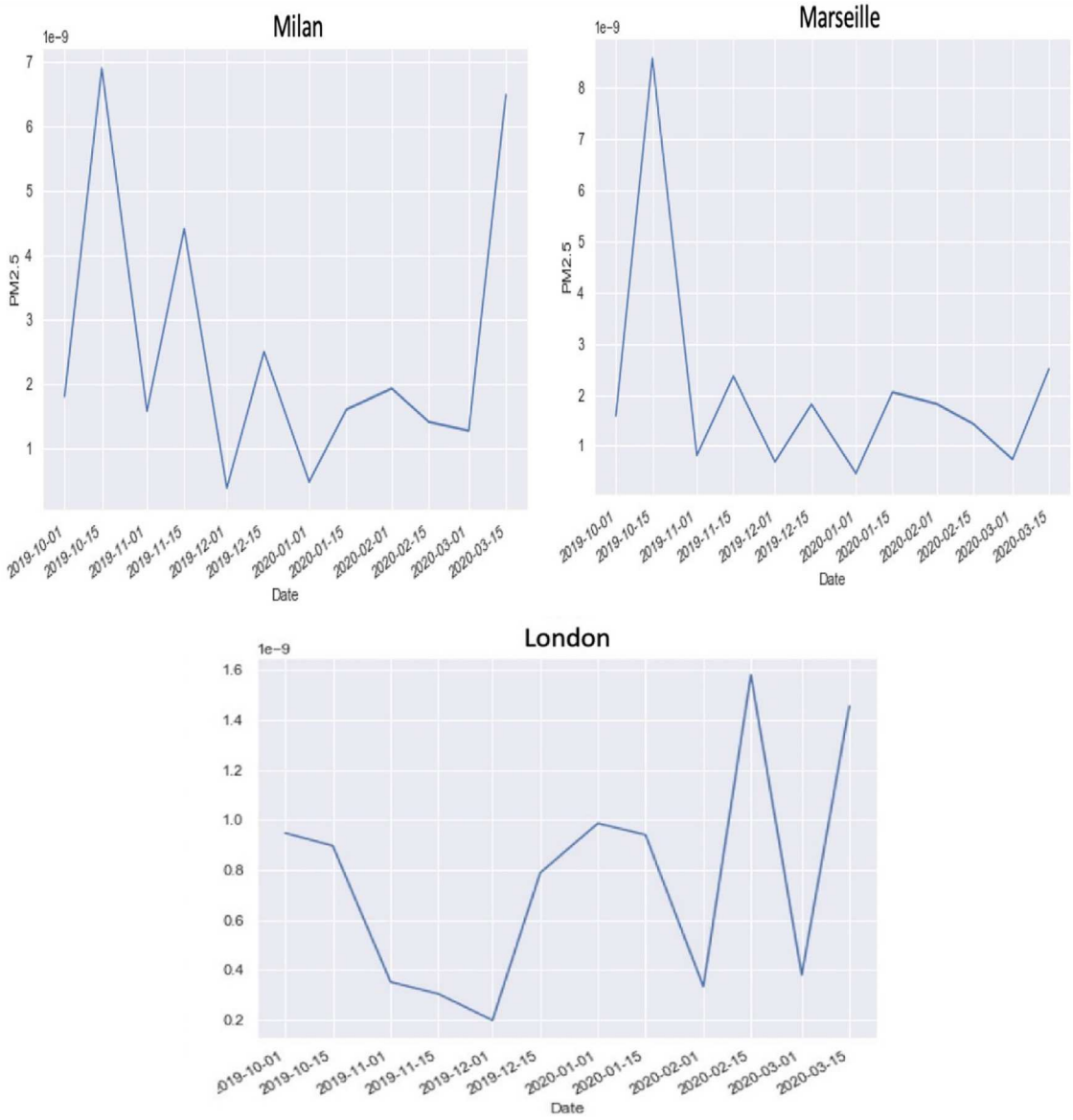

Fig. 11. Temporal change of $PM_{2.5}$ over Milan, Marseille, and London (Units are in kg/m3).

NO_2, $AOD_{500,}$ and UAI. India exhibited a prominent declining trend for AOD_{500} from November 15, 2019–January 31, 2020 ranging between 0.175 and 0.350, UAI from November 15, 2019–March 31, 2020, and $PM_{2.5}$ from November 1, 2019 to December 30, 2019. It showed a mixed trend for SO_2, O_3, and NO_2 (Fig. 8).

The nationwide lockdown started here on March 25, 2020. In India, the change in air quality was observed in two metro cities- NCR Capital (Delhi) and Mumbai. NCR Capital showed a declining trend in $PM_{2.5}$ over the study period from October 15, 2019–December 30, 2019 with the least concentration (<5 μg/m^3) from December 15, 2019–December 30, 2019 (Fig. 9). Mumbai showed (relatively) overall low concentration of $PM_{2.5}$ (<10 μg/m^3) with a peak from March 1, 2020–March 15, 2020. The NO_2 profile of Delhi NCR showed a decreasing trend from December 15, 2020 (Fig. 10). In Mumbai, initially, an increased pattern was observed reaching up to 0.7 molecules per cm^2, however, gradually the trend declined and reached below 0.4 molecules per cm^2 in the mid-March 2020 during the lockdown period. Iran overall showed a declining trend in AOD_{500}, UAI, and NO_2, whereas a mixed trend for $PM_{2.5}$, SO_2, and O_3. The same increasing pattern in $PM_{2.5}$ was observed in Istanbul from March 1, 2020 (Fig. 9).

3.1.4. Europe

In Europe, Germany showed a declining trend in AOD_{500} and NO_2 from October 1, 2019. UAI shows a mixed pattern ranging from 0.2 to 0.6 with a prominent drop on December 1, 2020, with a trough below 0.20. During the study period, $PM_{2.5}$ in Germany was within 2 μg/m^3. There is a distinct drop in SO_2 concentration from November 1, 2019–March 31, 2020, whereas O_3 shows an increasing trend till March 15, 2020. Stuttgart in Germany showed an overall low $PM_{2.5}$ concentration (<3 μg/m^3) throughout the study period. Spain and France show a mixed trend for all the parameters. France showed a similar pattern for UAI with the same range from 0.20 to 0.60. However, in France, Marseille showed a distinct declining trend in $PM_{2.5}$ from October 15, 2019 with a concentration <2 μg/m^3 mostly during January 2020 (Fig. 11). London also showed a decrease in $PM_{2.5}$ after October 15, 2019 and reported an overall increase mostly during winter (December 2019–January 2020) and early spring (February 2020–April 2020).

When investigated in Spain, Madrid showed a similar trend with an overall low concentration of $PM_{2.5}$ (<6 μg/m^3) from October 1, 2019–March 15, 2020. The NO_2 profile of Berlin and Barcelona shows a mixed pattern, ranging from 3.75 molecules per cm^2 to 5.50 molecules

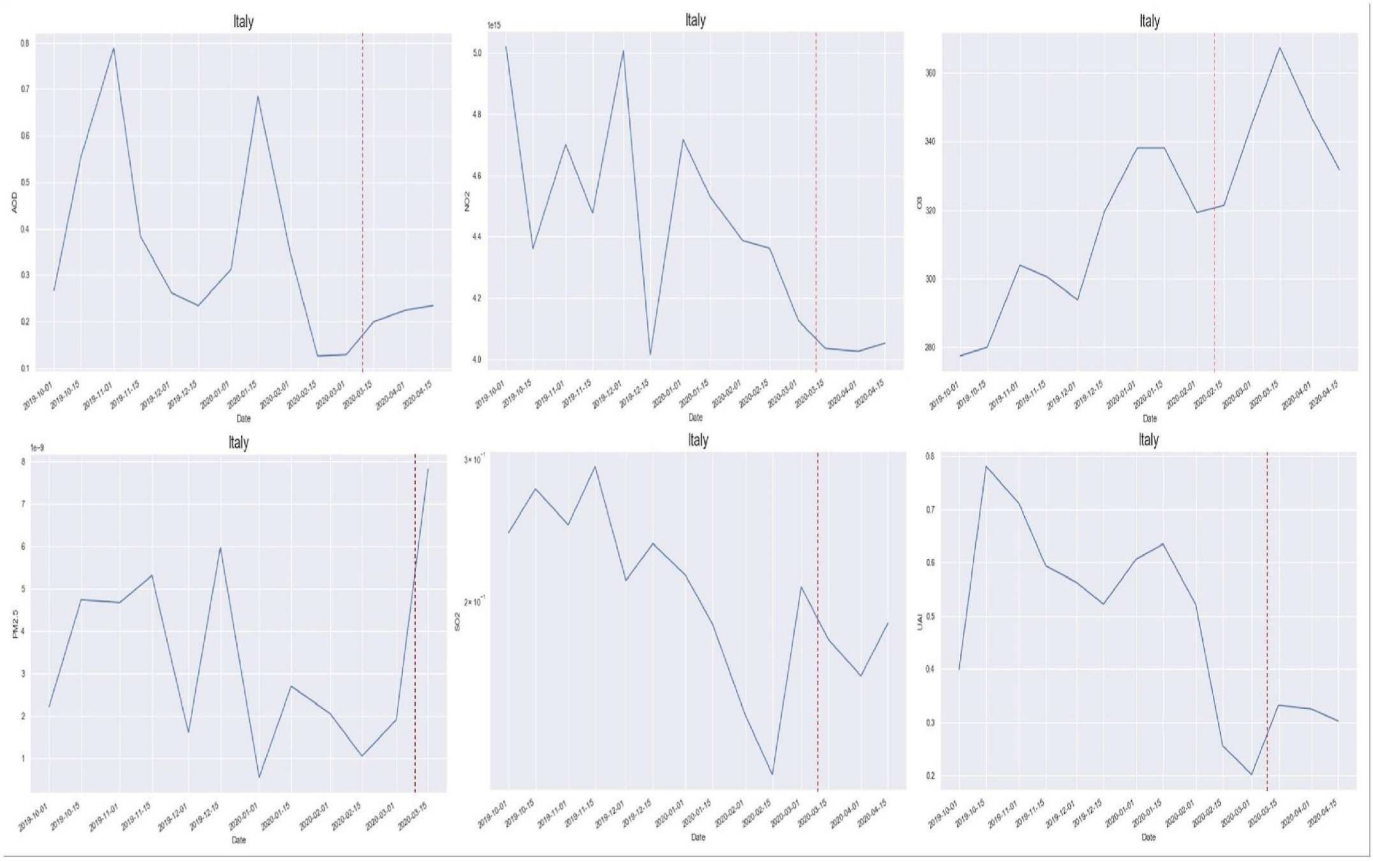

Fig. 12. Temporal change of six air quality parameters in Italy. The red vertical line indicates the lockdown date.

per cm^2 and 4.5 molecules per cm^2 to 8.0 molecules per cm^2. Similar to Spain and France, Italy also shows a mixed pattern (Fig. 12). However, there was a decreasing trend in NO_2, SO_2, and UAI from March 15, 2020 in Italy (just after the lockdown on March 9, 2020). Two cities in Italy, i.e. Milan and Napoli showed mixed trends in $PM_{2.5}$ concentration typically <7 $\mu g/m^3$ (Fig. 11). A country-wide mixed pattern for Italy was observed for the NO_2 profile from October 1, 2019 with a peak reaching 5.0 molecules per cm^2 on December 1, 2019 (Fig. 12). During the lockdown period in Italy, the national NO_2 profile showed a gradual decreasing trend reaching approximately 4.0 molecules per cm^2 on April 15, 2020. In both Marseille and London, NO_2 profile readings went up in March 2020 while Milan recorded a decreasing trend during the same period (Fig. 13).

3.1.5. North America

In North America, the United States (USA) showed a gradual declining pattern for UAI, and a mixed pattern for $PM_{2.5}$, AOD_{500}, and O_3. (Fig. 14).

The trend of SO_2 shows a relatively constant pattern up to March 15, 2020 followed by a sudden increase afterward. AOD_{500} showed a noticeable drop on April 1, 2020. It was observed that in New York City, $PM_{2.5}$ level ranged from 0.6 to 1.3 $\mu g/m^3$ except for January 1, 2020 when $PM_{2.5}$ level reached below 0.6 $\mu g/m^3$. Los Angeles showed an overall mixed pattern with $PM_{2.5}$ ranging from 1.25 $\mu g/m^3$ to 3.00 $\mu g/m^3$ except on November 15, 2019, when the value reached below 1.25 $\mu g/m^3$. In Salt Lake City, $PM_{2.5}$ trend showed a mixed pattern, ranging from 1.5 $\mu g/m^3$ to 4.0 $\mu g/m^3$ (Fig. 15). Canada as a country showed a decreasing trend for UAI and a gradual increasing pattern for PM 2.5, NO_2, and O_3 whereas the city of Toronto showed a mixed pattern for UAI, $PM_{2.5}$, and NO_2, and an increasing trend for O_3 (Fig. 15). In Toronto, NO_2 ranged from 6.0 molecules per cm^2 to 9.5 molecules per cm^2 with a sudden drop noticed from March 1, 2020 to April 1, 2020.

3.1.6. South America

In South America, a lockdown was initiated in Brazil on March 24, 2020. Brazil showed a mixed pattern for AOD_{500}, $PM_{2.5}$, and O_3. NO_2 profile showed a gradually decreasing trend and reached below 2.3 molecules per cm^2 after April 1, 2020. In Brazil, $PM_{2.5}$ typically varied from 1 $\mu g/m^3$ to 5 $\mu g/m^3$ with the highest peak on March 1, 2020 when it reached more than 5.5 $\mu g/m3$. Almost a similar mixed trend of $PM_{2.5}$ was noticed over Rio De Janeiro and Sao Paulo cities. In Rio De Janeiro, $PM_{2.5}$ value varied from 0.2 $\mu g/m^3$ to 1.2 $\mu g/m^3$ whereas in Sao Paulo the level ranged between 0.4 $\mu g/m^3$ to 1.6 $\mu g/m^3$ (Fig. 11). In Chile, a mixed trend could be seen for AOD_{500} and UAI with a decreasing trend for O_3. $PM_{2.5}$ also showed a mixed trend with a sudden notable drop below 0.8 $\mu g/m^3$ on January 15, 2020 and a peak reach of above 1.2 $\mu g/m^3$ on February 1, 2020. Initially, the NO_2 profile showed an increasing trend up to December 1, 2020 but gradually it declined and reached below 2.6 molecules per cm^2. In Santiago, $PM_{2.5}$ levels showed mixed patterns ranging from 0.8 $\mu g/m^3$ to 1.6 $\mu g/m^3$ (Fig. 11).

3.2. Phase II: all-level comparison of $PM_{2.5}$ and NO_2 responses between March–April 2019 and March–April 2020

As per available reports and online sources (https://www.bbc.co.uk/news/world-52103747), the majority of the countries imposed their lockdown during mid to late March 2020, which continued till April 2020, except for a few countries. For example, in Wuhan (in China) the lockdown took place during 3rd February – February 24, 2020. In Rome (in Italy) lockdown period was during 9th March – March 30, 2020

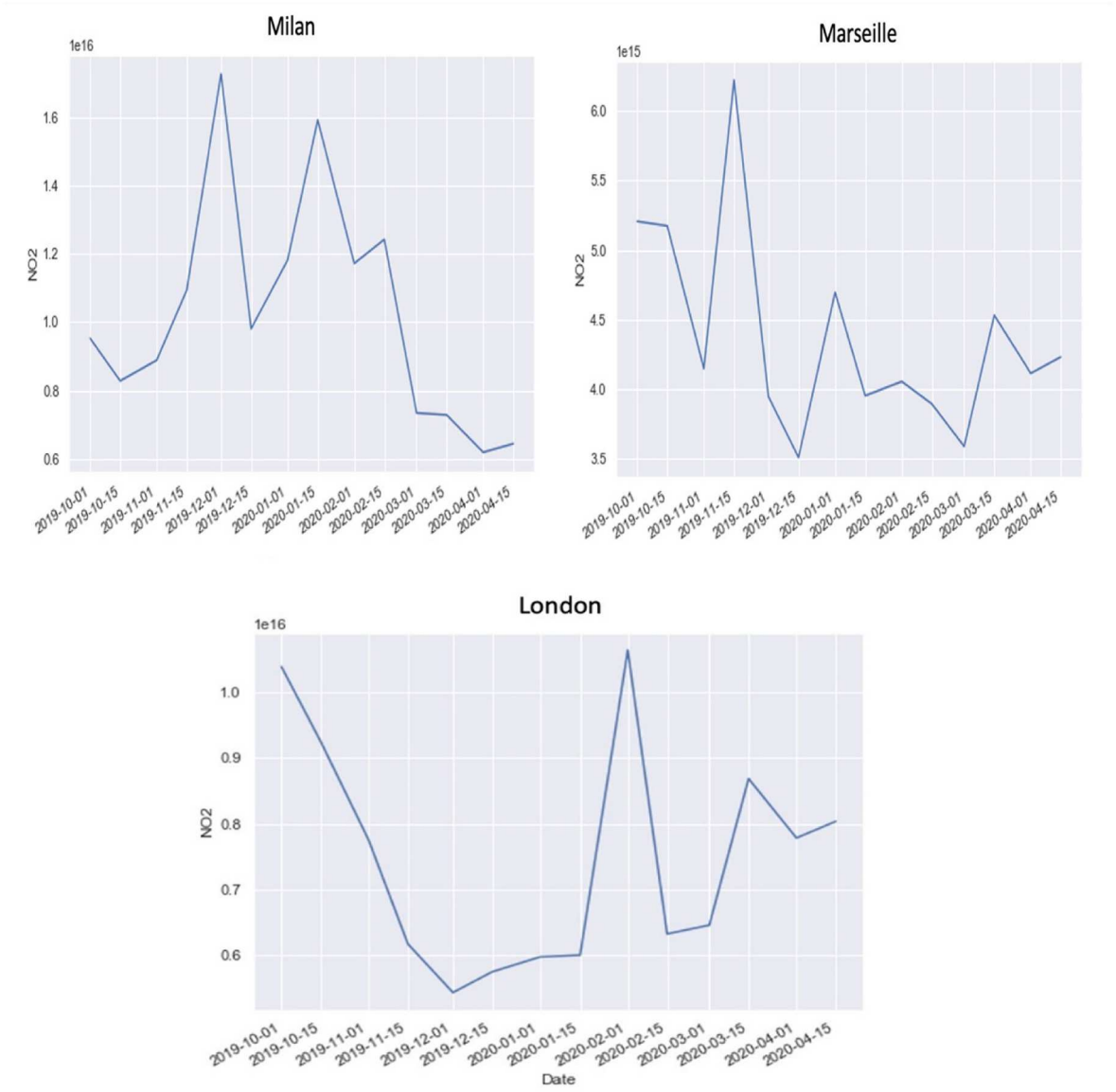

Fig. 13. Temporal change of NO_2 over Milan, Marseille, and London (Units are in molecules per cm^2).

(IQAir). In some countries, however, the lockdown period continued beyond April 2020. Hence, to analyze pre-lockdown and post-lockdown impacts on air quality, the response of two of the most important pollutants i.e. particulate matter ($PM_{2.5}$), and nitrogen dioxide were measured for the months of March–April 2019 and March–April 2020.

3.2.1. *Response of $PM_{2.5}$*

The study observed the mean national concentration of $PM_{2.5}$ for some randomly selected countries and cities that fall within and observed the range of $PM_{2.5}$ within the timeframe of 15th March – 30th April, both in 2019 and 2020. Following this, the percentage change in their mean, minimum, and maximum value were calculated (Table 5). Although in the previous analysis (Phase I), many of the cities showed a mixed trend when observed over a continuous time interval from October 2019 to April 2020, however, when compared with the lockdown period in 2020 with the same period in 2019, most of the cities showed a declining pattern in mean $PM_{2.5}$ concentration except Rome, Madrid, and Los Angeles. Los Angeles initially showed a drop in $PM_{2.5}$ during March 2020 in comparison to 2019, however, it increases in April. Rome showed a noticeable increasing pattern in $PM_{2.5}$ in 2020 from the previous year. Although in March 2020 Madrid shows an increasing pattern in $PM_{2.5}$, but gradually in April 2020, the concentration of $PM_{2.5}$ declined in comparison to 2019 (Table 5).

The global distribution of $PM_{2.5}$ from April 15, 2019 to April 30, 2019 in selected 20 countries is shown in Fig. 16a. The value of $PM_{2.5}$ ranges from 0.74 μg/m^3 to 54.7 μg/m^3, wherein many countries have their $PM_{2.5}$ values within the permissible limit mentioned by WHO (<10 μg/m^3), namely Canada, Russia, USA, South Africa, Brazil, Chile, France, Mexico, Spain, and Australia.

In Asia, Iran, China, India, and Turkey had higher $PM_{2.5}$ concentrations with respect to the permissible limit in the last 15 days in April 2019. In Africa, Ghana, and Egypt show the maximum concentration of $PM_{2.5}$, 33.30 μg/m^3, and 54.70 μg/m^3 respectively.

In contrast to 2019, it is observed that many countries which have previously high $PM_{2.5}$ concentrations have shown reduced levels of $PM_{2.5}$ in 2020 (Fig. 16b).

The value of $PM_{2.5}$ ranges from 0.73 to 49.13 μg/m^3. Italy and Turkey have entered the permissible limit, with a reduced $PM_{2.5}$ value of 5.15 and 5.62 μg/m^3, whereas Ghana has a $PM_{2.5}$ value of 44.03 μg/m^3, which has increased from the previous year. Changes in averaged $PM_{2.5}$

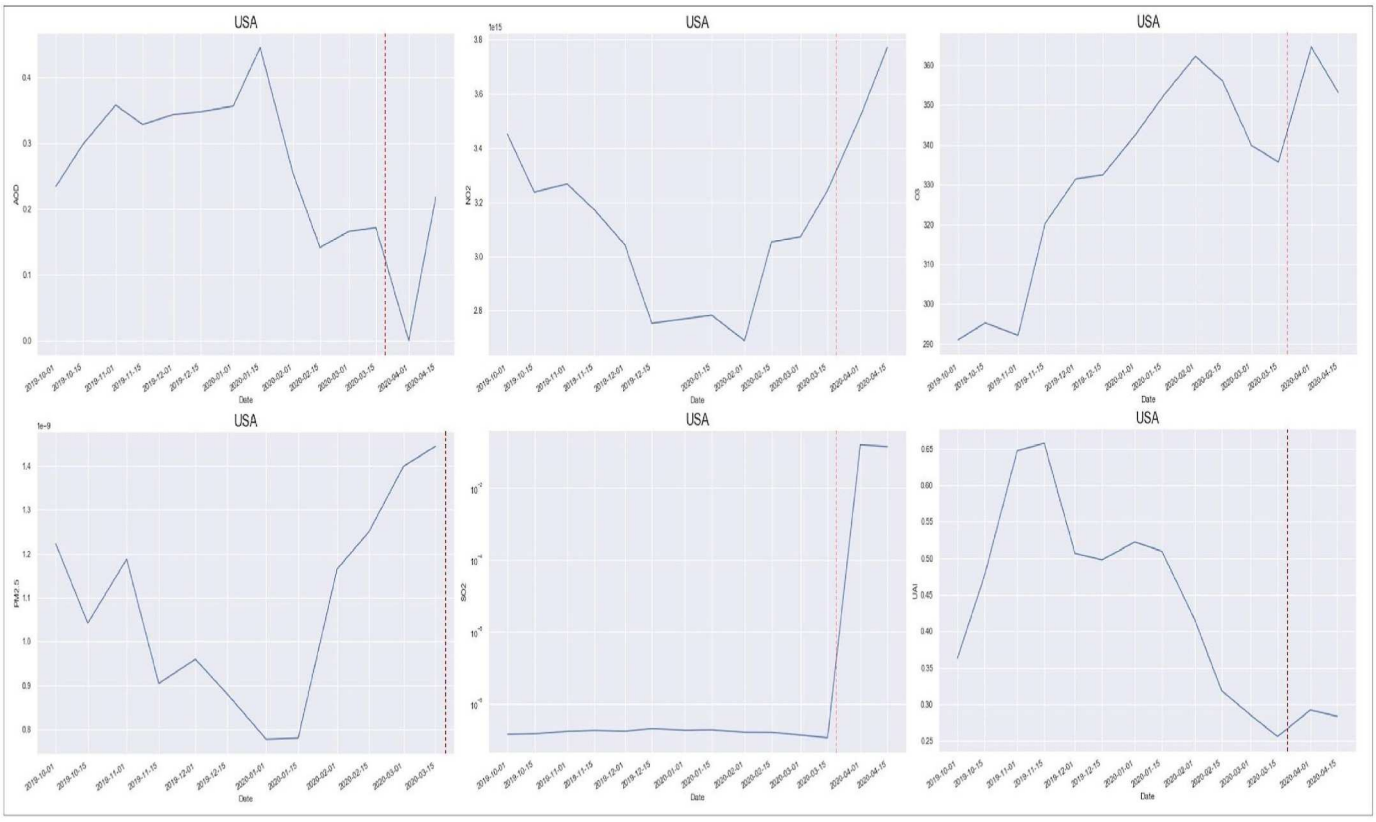

Fig. 14. Temporal change of six air quality parameters in the USA. The red vertical line indicates the lockdown date.

from 2019 to 2020 are shown in Fig. 17.

Results show that due to constrained human activities and dropped anthropogenic emissions (Li et al., 2020a), $PM_{2.5}$ concentration has reduced by 56% in 2020 compared to the previous year. A maximum reduction of $PM_{2.5}$ concentration by 6.46 μg/m^3 is observed in Italy with a relative reduction of 56%. On the contrary, some cities recorded increased $PM_{2.5}$ concentrations ranging from 4 to 110%. A maximum increase of $PM_{2.5}$ concentration by 10.73 μg/m^3 is observed in Ghana, although a maximum relative $PM_{2.5}$ increase of 110% is observed in Russia.

While investigating at the city level, the change of $PM_{2.5}$ during 2019 and 2020 for the same period has been analyzed and presented in Table 5. Brazil observed a reduction in $PM_{2.5}$ concentration up to 62.74% and 14.94% during 15 March – 31 March and 15th April – 30th April at a country level. During 23rd March – 13th April and 1st April – 15th April there was an increase in $PM_{2.5}$ concentration was noticed. In China, during 1st February – 15th February, there was a reduction in $PM_{2.5}$ by 26.42%, however, it slightly increased from 3rd February to 24th February by 1.02% and 46.63% during 15th February – 28th February. In India, $PM_{2.5}$ has reduced significantly from 15th March – 31st March by 34.09%. It is further observed there is a change in $PM_{2.5}$ in 2020 in comparison to 2019 from 23rd March – 13th April (-24.83%), 1st April – 15th April (-12.55%), and 15th April-30th April (-13.55%). Italy overall showed a sudden increase in $PM_{2.5}$ during 9th March – March 30, 2020 by as high as 539.34% in comparison to the same time period in 2019. Similarly in Spain, when comparing with 2019, a positive change in $PM_{2.5}$ concentration in 2020 from 15th March - 31st March (344.64%), 23rd March – 13th April (72.18%), and 1st April – 15th April (147.23%), 15th April – 30th April (-5.08%) was observed. The study also showed an overall drop in $PM_{2.5}$ in the UK in 2020 when compared with 2019. The change in $PM_{2.5}$ observed in the UK from 15th March – 31st March was lower by -0.61%, and that of 15th April – 30th April was lowered by -47.19%. In the USA no such reduction in $PM_{2.5}$ was noticed in comparison to 2019 except from 15th March – 31st March with a reduction rate of 5.68%.

3.2.2. *Response of NO_2*

Similar to $PM_{2.5}$, the mean national percent change and the max-min range of NO_2 for the same randomly selected countries and cities were observed for the same timeframe. The date-wise and location-wise details of NO_2 concentration change between 2019 and 2020 have been illustrated in Table 6.

Fig. 18 shows the global distribution of NO_2 for the duration of 15th April - 30th April for the years 2019 and 2020.

Overall, the value of NO_2 ranges from $0.24 \times 10^{16}\ cm^{-2}$ to $0.66 \times 10^{16}\ cm^{-2}$. In 2019, Brazil had the minimum NO_2 concentration ($0.24 \times 10^{16}\ cm^{-2}$), whereas Germany had the maximum NO_2 concentration ($0.66 \times 10^{16}\ cm^{-2}$). In 2020, while there was no significant change in the (global) lower limit of NO_2 concentration, a drop in the global upper limit of NO_2 was seen. In 2020, the NO_2 concentration ranged from $0.22 \times 10^{16}\ cm^{-2}$ to $0.51 \times 10^{16}\ cm^{-2}$. It is observed that most of the countries had shown a decreasing pattern in the NO_2 profile during the lockdown period. Fig. 19 showed the global change in NO_2 concentration in 20 selected countries.

Results showed that due to the constrained vehicle movement, industrial emissions, power plants, construction works, and agricultural

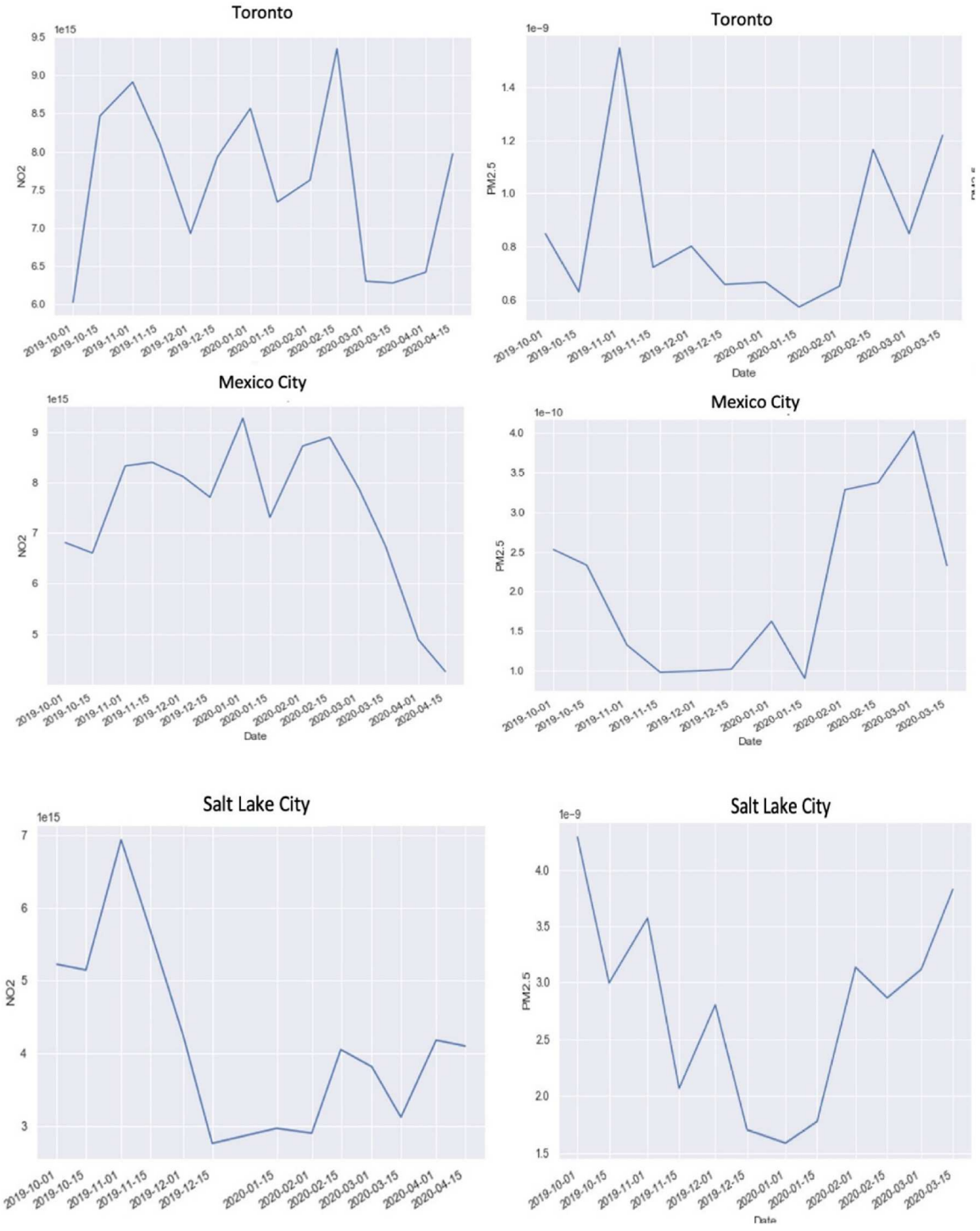

Fig. 15. Temporal change of NO_2 and $PM_{2.5}$ over some North American cities (Units are in molecules per cm for NO_2, and kg/m3 for $PM_{2.5}$).

Table 5
Percentage change in $PM_{2.5}$ in randomly selected countries and cities from 2019 to 2020.

Country	City	Interval	Mean change (%)	Minimum change (%)	Maximum change (%)
Brazil	Sao Paulo	15 Mar-31 Mar	7.56	9.34	36.79
		23 Mar-13 Apr	-28.06	-24.2	-13.03
		01 Apr-15 Apr	-20.05	-16.68	-5.28
		15 Apr-30 Apr	-11.23	-11.38	4.65
China	Shanghai	01 Feb-15 Feb	-49.76	-50.45	-45.88
		03 Feb-24 Feb	-36.63	-39.81	-29.77
		15 Feb-28 Feb	5.28	3.55	14.85
	Wuhan	01 Feb-15 Feb	-55.11	-46.87	-29.64
		03 Feb-24 Feb	-38.91	-32.05	-18.08
		15 Feb-28 Feb	21.58	33.75	33.2
India	Mumbai	15 Mar-31 Mar	-40.7	-39.62	-29.91
		23 Mar-13 Apr	-4.64	-296	1.93
		01 Apr-15 Apr	27.29	24.74	33.19
		15 Apr-30 Apr	-12.9	-11.24	-1.38
	NCR Capital	15 Mar-31 Mar	-14.96	-14.86	-7.39
		23 Mar-13 Apr	-31.6	-32.64	-28.38
		01 Apr-15 Apr	-26.3	-25.68	-22.12
		15 Apr-30 Apr	-25.52	-26.71	-19.81
Italy	Rome	09 Mar-30 Mar	494.72	494.72	494.72
Spain	Madrid	15 Mar-31 Mar	568.24	616.51	549.18
		23 Mar-13 Apr	91.81	106.79	108.66
		01 Apr-15 Apr	157.06	133.51	197.83
		15 Apr-30 Apr	-25.84	-21.3	0.46
UK	London	15 Mar-31 Mar	19.17	19.17	19.17
		23 Mar-13 Apr	66.45	66.45	66.45
		01 Apr-15 Apr	7.53	7.53	7.53
		15 Apr-30 Apr	-31	-31	-31
	Manchester	15 Mar-31 Mar	-21.11	-21.13	-8.2
		23 Mar-13 Apr	87.64	77.92	98.56
		01 Apr-15 Apr	23.18	21.65	26.07
		15 Apr-30 Apr	-53.34	-51.73	-46.23
USA	Los Angeles	15 Mar-31 Mar	-35.57	-6.88	19.42
		23 Mar-13 Apr	9.13	36.86	47.22
		01 Apr-15 Apr	42.76	64.03	70.89
		15 Apr-30 Apr	20 36.81	74.44	81.54

activities, the level of NO_2 had decreased significantly by 31% compared to 2019 (Li et al., 2020b).

A maximum reduction of NO_2 concentration of $0.31 \times 10^{16}\ cm^{-2}$ was observed in the UK with a relative reduction of 32% from the previous year (2019). On the contrary, South Africa had shown a slight increase in NO_2 concentration of $0.005 \times 10^{16}\ cm^{-2}$ (1.35%).

3.3. Phase III: city-level comparison of air quality parameters during the first 15 days of April 2020 and the last 15 days of April 2020

In this phase, changes in AOD_{500}, NO_2, and O_3 concentrations over the selected cities in the last 15 days of April 2020 (15th April – April 30, 2020) were compared to the first 15 days of the same month (1st April – April 15, 2020).

Out of 37 selected cities, 13 cities showed a declining trend in AOD_{500}. The highest decline in AOD_{500} was observed in Johannesburg. Other cities that showed noticeable decreases in AOD_{500} are Pretoria, Riyadh, Mecca, London, Wuhan, Santiago, Berlin, Mumbai, and Istanbul.

Salt Lake City and Los Angeles showed an increasing trend in AOD_{500} followed by Cairo and NCR Capital (Delhi), Milan, Shanghai, Beijing, Stuttgart, Sydney, Mexico City, and Tehran (Fig. 20).

In terms of NO_2, 16 cities showed a declining trend with the highest decline in Beijing followed by Stuttgart, Melbourne, Wuhan, Mexico City, Napoli, and Tabriz. However, Johannesburg and Pretoria showed an increasing NO_2 trend in the last 15 days in April followed by Tehran, Toronto, Hamilton, NCR Capital (Delhi), Madrid, and Sao Paulo. Both the UK cities, London and Manchester show an increasing trend in NO_2.

Out of 37 cities, 22 cities showed a prominent drop in O_3 concentration from 15th April – April 30, 2020 with the highest drop in Salt Lake City, Los Angeles followed by Ankara, Istanbul, Beijing, Napoli, NCR Capital (Delhi), Barcelona, Sydney, Melbourne. On the other hand, Manchester, London, Paris, Berlin, Stuttgart, Johannesburg, Toronto, and Hamilton showed increasing trends in O_3.

3.4. Validation

It is important to validate the results derived from remote sensing observations to ensure the reliability of the collected data and the accuracy of the results. Hence, as mentioned in the methodology section, we study compared the remotely sensed $PM_{2.5}$ mean percent change between 2019 and 2020 with IQAir ground-based monitoring data for the period of 15th March to 30th April (Table 7).

The common dates of both ground-based and satellite observations have been statistically compared with Pearson correlation (Pearson's Correlation Coefficient, 2008). The common observation dates were found between 23rd March to 13th April for the cities like Sao Paulo, Mumbai, NCR Capital, and Los Angeles. For Wuhan, the common observation date was from 3rd February to 24th February. The dates were chosen as they fall within the lockdown periods in the respective cities based on IQAir published report (IQAir). The Pearson correlation test showed good agreement between ground and satellite-based observation with $R^2 = 0.55$, $R = 0.75$ for the cities like Wuhan, Mumbai, NCR Capital, Sao Paulo, and Los Angeles (Fig. 21). All these cities

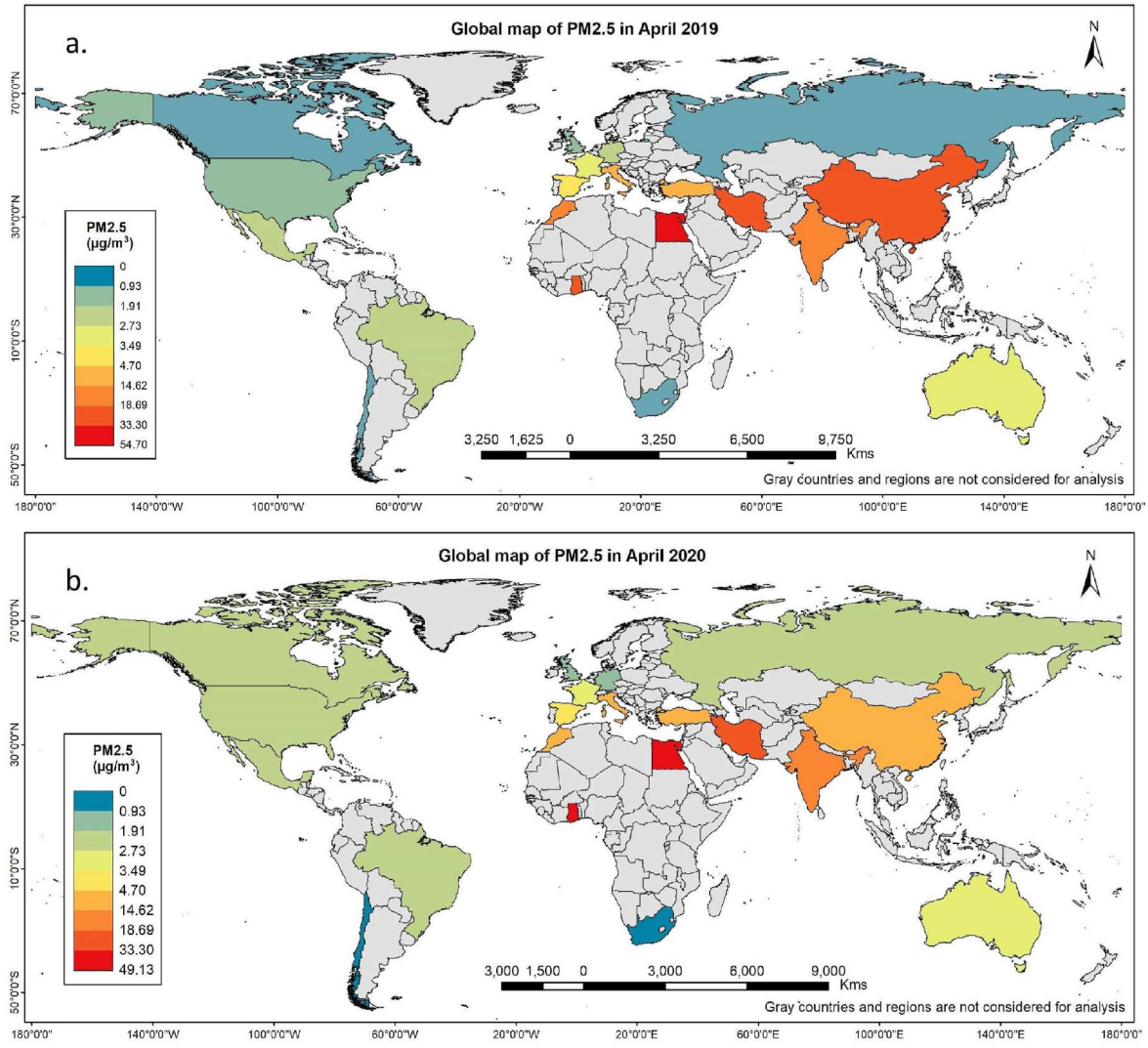

Fig. 16. Global maps of $PM_{2.5}$ concentration in (a) April 2019 and (b) April 2020.

showed a significant reduction in $PM_{2.5}$ using both ground-based and spaceborne observations. However, cities like London, New York, and Madrid have shown the opposite measurements from these two data sources. They had shown increasing numbers in the $PM_{2.5}$ level for s satellite observation while reducing numbers for ground-based measurements (Table 7). The reasoning behind this discrepancy can be justified as spaceborne measurements have coarser spatial resolution and are not as precise as ground-based measurements, introducing some spatial and spectral uncertainties. Due to a lack of ground-based country-level data, it was not possible to compare the change in country-level observations from satellite data with the ground-based measurements.

4. Discussion

This research successfully carried out detailed monitoring and analysis of global air quality through five major air quality parameters, i. e. NO2, $PM_{2.5}$, O3, AOD_{500}, UAI, and in some cases SO_2 for pre, post, and during COVID-19 lockdown situations. It adopted a top-down approach from country to city level (urban agglomeration) and showed how dynamically the air quality parameters had changed at various spatial levels. Countries like China, India, Mexico, South Africa, Italy, Spain, and Australia have shown decreasing trends for $PM_{2.5}$ in 2020 as compared to 2019, whereas countries like Canada, the USA, and Russia have shown increasing trends for $PM_{2.5}$ in 2020 compared to 2019. Similarly, NO_2 decreased in 2020 in most of the countries, for example, in Italy, Spain, Germany, UK, the USA, Russia, India, Mexico, China, Australia, Brazil, whereas South Africa showed an increasing NO_2 trend.

European cities like Rome, Madrid, London, and Manchester had experienced an increasing trend of $PM_{2.5}$ mostly from 15th March to 15th April probably due to the reliance on residential heating systems which generally work till mid of April, coupled with cool air inversions that trap particulate pollution in the atmosphere. This may explain $PM_{2.5}$ gains in some of the cities when observing through spaceborne remote sensing systems. Studies also reported that in most European cities people have been exposed to higher levels of $PM_{2.5}$ pollution indoors because more time spent cooking at home executes higher emissions of $PM_{2.5}$. In the UK, pollutants from northern Europe through easterly winds added to UK emissions along with higher temperatures in UK cities leads higher $PM_{2.5}$ concentrations during the lockdown period. However, the reduction in NO_2 levels in Germany, the UK, Italy, and Spain can be justified by less usage of vehicles and lower activities in industrial and manufacturing plants.

Chinese cities like Wuhan and Shanghai exhibited a reduced trend of $PM_{2.5}$ in 2020 compared to 2019 due to lockdown measures. However, after the post-lockdown period at the end of February 2020, there had been an increase in $PM_{2.5}$ in China. Though road traffic emissions may

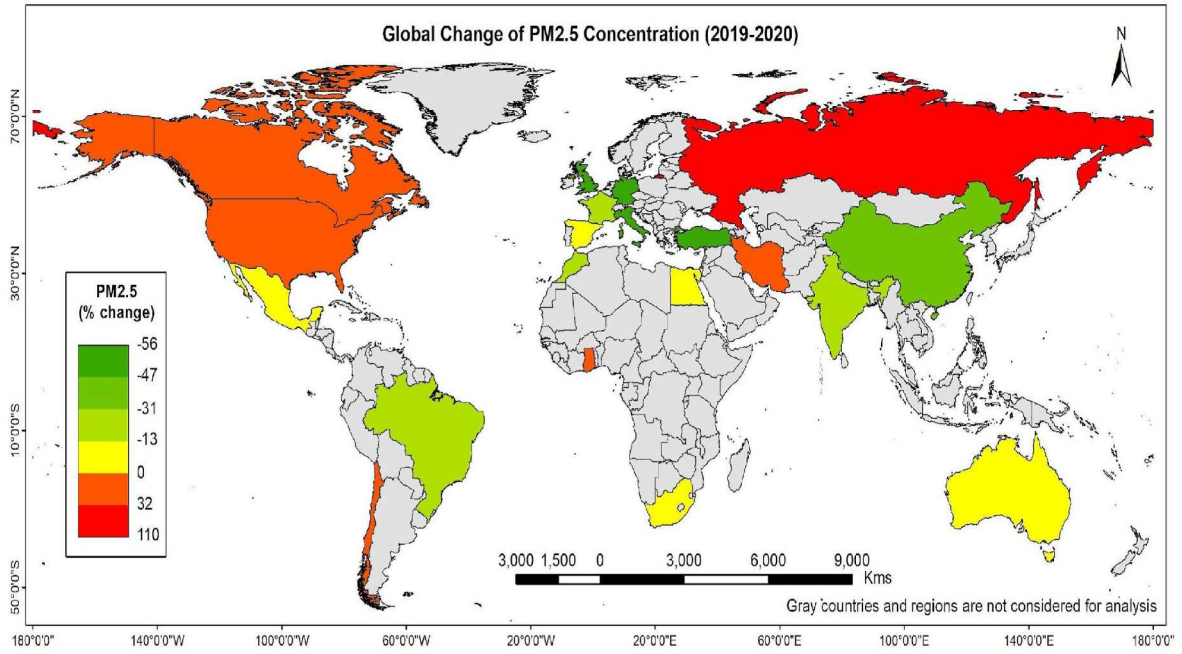

Fig. 17. Global change of $PM_{2.5}$ concentration between April 2019 and April 2020.

Table 6
Percentage change in NO_2 in selected countries from 2019 to 2020.

Country	Interval	% Mean Change	% Minimum Change	% Maximum Change
Brazil	15 Mar-31 Mar	-62.74	-33.44	33.72
	23 Mar-13 Apr	4.57	-26.82	84.79
	01 Apr-15 Apr	57.59	-13.17	100.58
	15 Apr-30 Apr	-14.94	-2.89	83.77
China	01 Feb-15 Feb	-26.42	126.83	104.37
	03 Feb-24 Feb	1.02	157.04	98.13
	15 Feb-28 Feb	46.63	62.66	130.35
India	15 Mar-31 Mar	-34.09	-38.76	62.01
	23 Mar-13 Apr	-24.83	-9.3	71.05
	01 Apr-15 Apr	-12.55	-6.28	83.24
	15 Apr-30 Apr	-13.35	-68.18	94.22
Italy	09 Mar-30 Mar	539.34	190.04	283.79
Spain	15 Mar-31 Mar	344.64	470.99	193.47
	23 Mar-13 Apr	72.18	197.42	70.93
	01 Apr-15 Apr	147.23	292.68	195.48
	15 Apr-30 Apr	-5.08	67.09	84.67
UK	15 Mar-31 Mar	-0.61	28.96	106.73
	23 Mar-13 Apr	84.21	76.49	108.18
	01 Apr-15 Apr	24.69	46.25	62.33
	15 Apr-30 Apr	-47.19	-53.3	7.48
USA	15 Mar-31 Mar	-5.68	-22.85	57.03
	23 Mar-13 Apr	15.2	13.04	60.99
	01 Apr-15 Apr	28.05	28.86	66.29
	15 Apr-30 Apr	23.63	52.2	75.83

not have contributed to the sudden increase of $PM_{2.5}$, but industrial emissions outside the cities could have added to the emission levels.

In India, a significant reduction in $PM_{2.5}$ and NO_2 can be noticed due to strict lockdown measures and stay-at-home orders for the 1.3 billion population. Measures like shuttered businesses, no traffic congestion, paused construction projects, closed non-essential industries, vehicle free roads accelerated the process of reduction in $PM_{2.5}$ and NO_2. The major Indian cities, for example, Mumbai, NCR Capital (Delhi) had also experienced reduced $PM_{2.5}$ levels during lockdown situations, that started on March 25, 2020.

In the USA, during the lockdown, the Federal government rolled back emissions standards and relaxed certain environmental policies (Holden, 2020). This may be a reason behind the increasing trend of $PM_{2.5}$ (Barret, 2020). Besides, the continuous operation of power plants during lockdown might also be a reason for increased $PM_{2.5}$ in USA (Schiermeier, 2020).

In Brazil, local meteorology and seasonal forest fire in the Amazon might be a reason behind the national increasing trend of $PM_{2.5}$. Low traffic flow in the overall country might have helped reduce the NO_2 concentration of the country.

The power plants, and waste treatment plants around the cities, and their continuous emission may also have varyingly impacted the

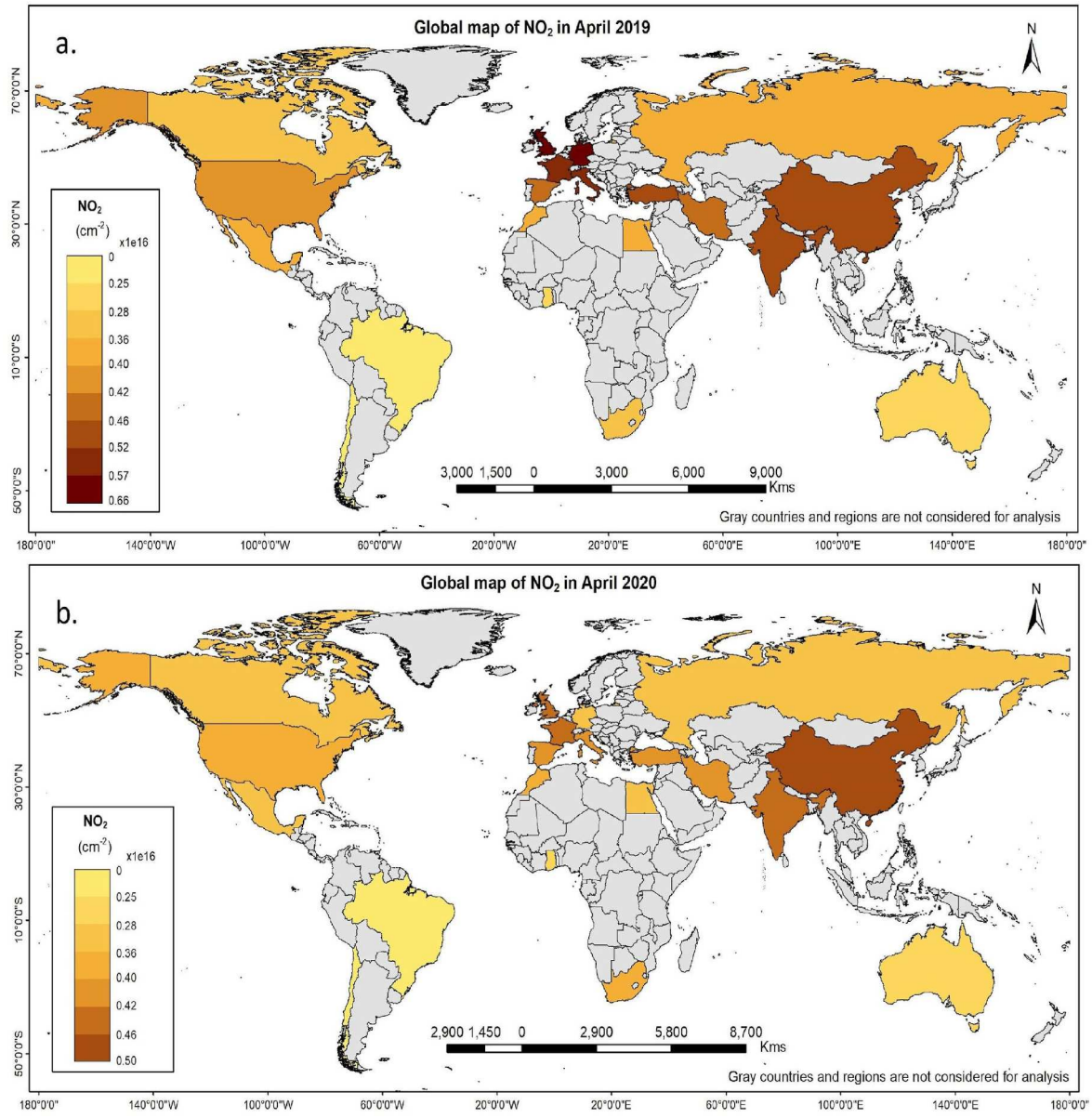

Fig. 18. Global maps of NO_2 concentration in (a) April 2019 and (b) April 2020.

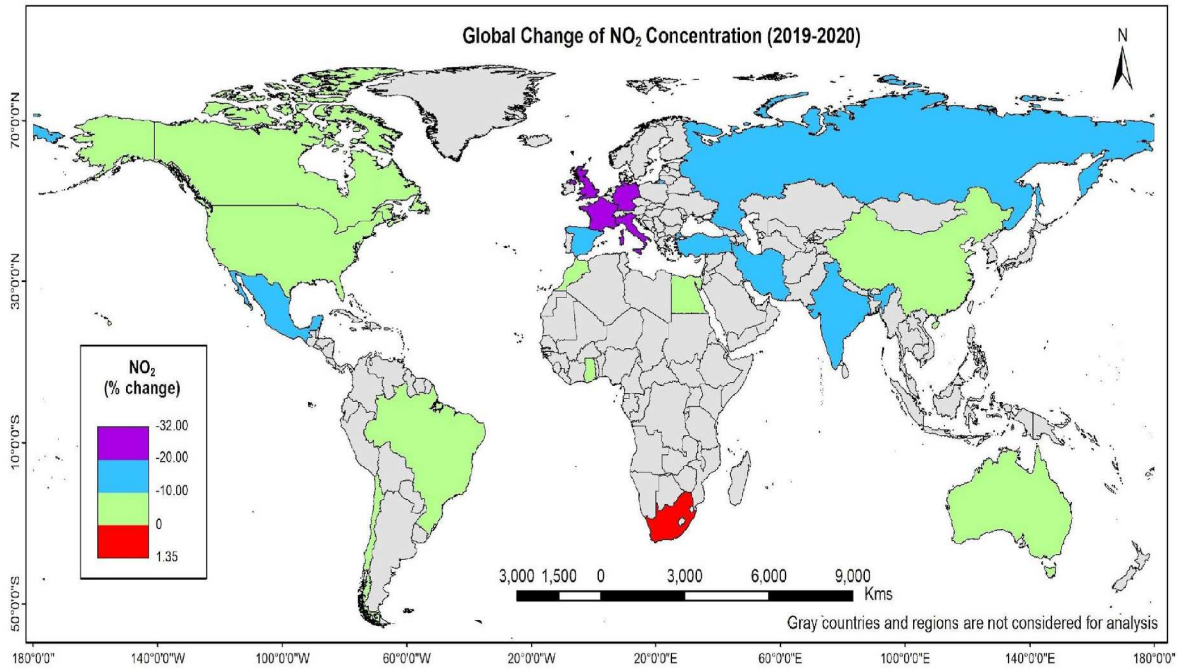

Fig. 19. Global change of NO_2 concentration between April 2019 and April 2020.

pollution level of the cities since these remained operational even during lockdowns.

This study observed that there is spatial variability in air quality even within a country. Some parts of a country show good air quality (low concentration of pollutants) whereas some parts had comparatively poor air quality, especially in the industrial zones. For example, from 15th April - April 30, 2020, while most part of Italy shows a low concentration of NO_2, the northern part, e.g., Milan, Veneto, and Emilia-Romagna, which involves large industrial activities, shows a higher concentration of NO_2 (Fig. 22b). The same pattern can be observed for $PM_{2.5}$ during late March 2020 as well (Fig. 22a).

In Germany, Ruhr and the surrounding region in North Rhine-Westphalia, the center of different industrial activities (e.g., automobile, coal, and steel plants), show higher concentrations of NO_2. The eastern part of Germany shows comparatively low NO_2 concentration in April 2020. Fig. 23 shows a gradual decline in NO_2 in Germany from February to April 2020.

Likewise, in South Africa, since the major industries are located in its eastern part, a very prominent NO_2 concentration in that region was observed (Fig. 24) that increased in 2020.

Due to such spatial variability, there may be cases when a given city showed a drop in a few air quality parameters whereas the entire country measured an increase in air pollution levels.

5. Conclusion

As mentioned earlier, most of the published studies investigating air quality change during the COVID-19 lockdown period are city-based studies, considering administrative city boundaries. Their analysis did not include the power plants, coal mines, water treatment plants, and other essential and active services beyond the city limits which continuously emitted $PM_{2.5}$, NO2, and other pollutants. These sites were operated 24/7 to ensure normalcy for citizens lives who were all staying indoors during the lockdown period. Given the enormous impacts these establishments have on local as well as regional air pollution levels and dispersion, it is imperative to take them into consideration while assessing the air quality of any region. As to the knowledge of the authors, this study is the first to address as well as rectify that oversight. This study also highlights the unjustified generalization of concluding that overall global air pollution decreased during the COVID-19 lockdown since not every part of the world responded the same way to the situation. In fact, dynamic response variations and mixed patterns were observed among different cities within the same country. With multi-layered top-down analysis, this study was able to access the variability in the global air quality at different levels of spatial granularity and busted the common belief that the overall global air quality had improved during the COVID-19 lockdown period. The study showed that local conditions have uniquely influenced the concentration of atmospheric pollutants. Hence, it is very difficult to generate an overall global air quality report for the COVID-19 regime since the conditions varied with space, time, and scale of observation. During the lockdown period, $PM_{2.5}$ concentrations had reduced by 56% in 2020 compared to 2019 in most countries except Ghana and Russia which showed increasing trends. The NO_2 concentration had also decreased by 3%–31% in most of the countries but some of them like Turkey and Spain showed a mixed pattern, whereas the UK and South Africa exhibited increasing trends. The region covered by NCR Capital (Delhi) in India showed a prominent declining trend in $PM_{2.5}$ value whereas in most parts, SO_2, AOD_{500}, and UAI presented a mixed pattern fluctuating over the study period. O3 increased in most of the countries (with some city-level variations). Reduced emissions from secondary industries and motor vehicles are most likely the cause behind the observed decrease in $PM_{2.5}$ and NO_2 during the lockdown period. The increased O_3 is probably due to lower particle loading that led to less foraging of hydroperoxyl radicals (HO_2) suggested by Wang (Wang et al., 2020). Ghana registered an overall increase of $PM_{2.5}$ but a decrease in NO_2 at the same time. These results

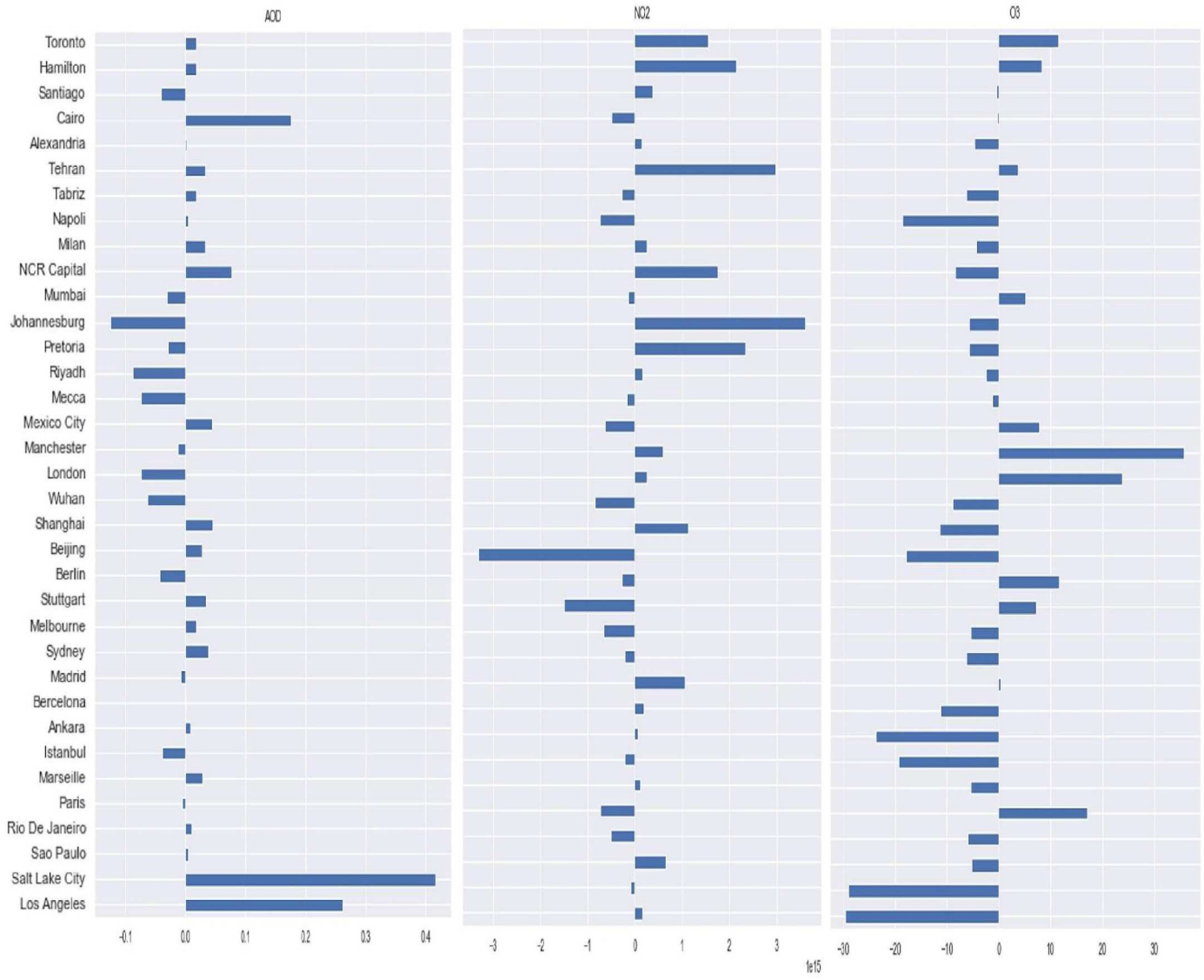

Fig. 20. Absolute change in AOD_{500}, NO_2, O_3 concentration in selected cities between 1st April – 15th April, 2020 and 15th April – 30th April, 2020.

Table 7
Comparison between satellite observation and ground observation (mean percent change of $PM_{2.5}$).

Country	City	Interval	Ground observation (IQAir) % Mean Change	Satellite Observation % Mean Change
Brazil	Sao Paulo	23 Mar-13 Apr	-54	-28.06
China	Wuhan	03 Feb-24 Feb	-44	-38.91
India	Mumbai	23 Mar-13 Apr	-34	-4.64
	NCR Capital	23 Mar-13 Apr	-60	-31.6
Italy	Rome	09 Mar-30 Mar	30	494.72
Spain	Madrid	23 Mar-13 Apr	-11	91.81
UK	London	23 Mar-13 Apr	-9	66.45
USA	Los Angeles	23 Mar-13 Apr	-31	9.13
	New York	23 Mar-13 Apr	-25	46.05

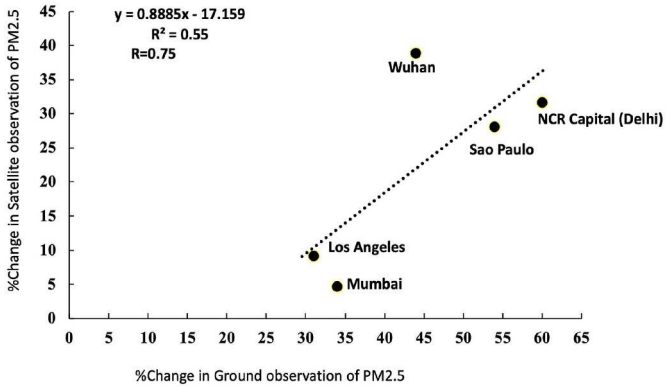

Fig. 21. Correlation between satellite observation and ground measurement.

clearly indicate that since there are many atmospheric pollutants or parameters that influence the quality of air, it is completely subjective to the scale of observation and what pollution parameters are being referred to when assessing the air quality standards. Air quality is also

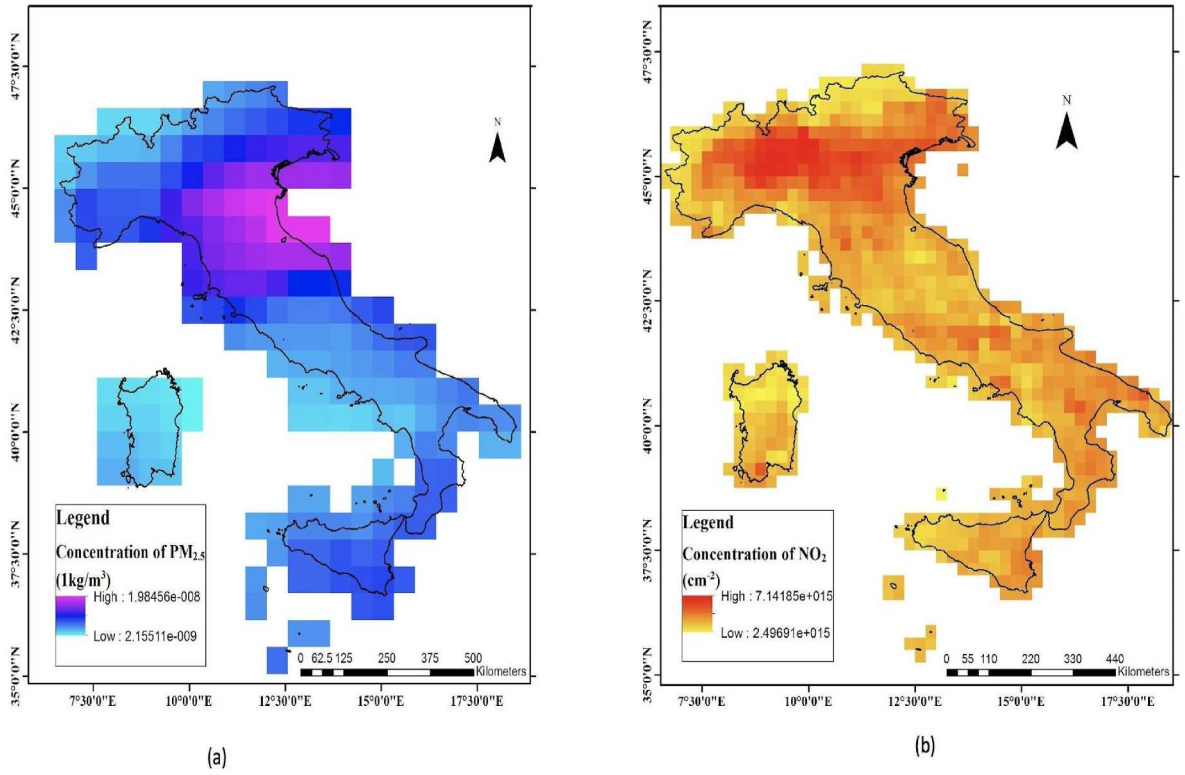

Fig. 22. (a) $PM_{2.5}$ and (b) NO_2 distribution in Italy in March 2020, April 2020 respectively.

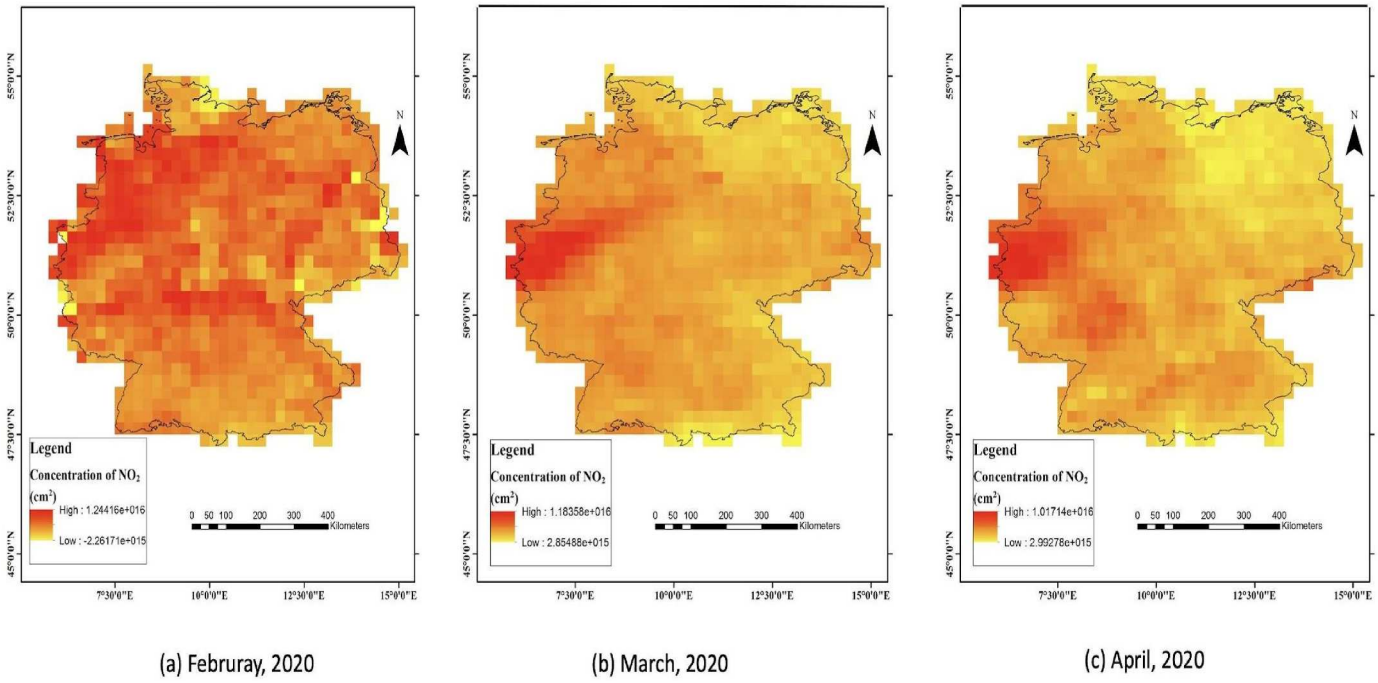

Fig. 23. Spatiotemporal variation in NO_2 over Germany from February to April 2020.

significantly controlled by weather phenomena, e.g., excessive rainfall, low temperature, wind speed, and solar influx (Borge et al., 2019). Hence, further study is required to understand the contribution of weather factors on air quality change during the COVID-19 lockdown. Future studies in this regard can also incorporate spaceborne and ground-based observations and develop a more comprehensive hybrid model to investigate changes in the air quality at different spatial and temporal scales over different land use and land cover type. The limitations of the present study are low spatial resolution, data gaps, and mixed pixel impurity problems (Hsieh et al., 2001). Therefore, a finer spatial resolution with a source-based study of air quality parameters is recommended to get a further detailed explanation of the lockdown on air quality scenario. However, even with the limitations mentioned above, the wide-scale satellite observation proved to have provided the

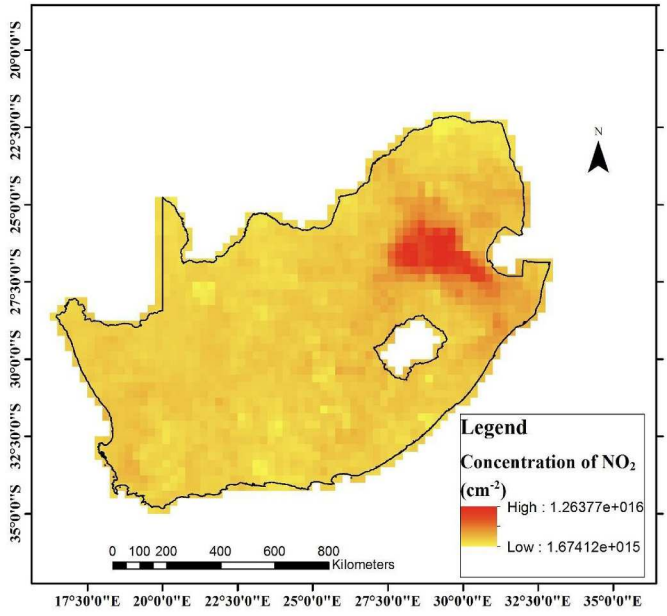

Fig. 24. Spatial variability of NO_2 in South Africa.

advantage of getting a synoptic view of air quality at any location where ground-based observation is not available.

Funding

This study was supported through the NASA Interdisciplinary Research in Earth Science (IDS) program (Grant No. NNH19ZDA001N-IDS).

Declaration of competing interest

Authors declare no conflict of interests.

Data availability

Data will be made available on request.

Acknowledgment

Analyses and spaceborne visualizations used in this study were produced with Google Earth Engine owned by Google LLC., and the NASA Giovanni online data system developed and maintained by the NASA GES DISC. We gratefully acknowledge the University of Southampton's Open Access and Institutional Repository Policy under no-cost-to-the-author publisher memberships and agreements. We would like to extend our appreciation to IQAir for providing open-source station data. Lastly, we would like to thank the anonymous reviewers for their valuable comments and feedback for the quality enrichment of the manuscript.

References

Abdullah, S., Mansor, A.A., Napi, N.N.L.M., Mansor, W.N.W., Ahmed, A.N., Ismail, M., Ramly, Z.T.A., 2020. Air quality status during 2020 Malaysia Movement Control Order (MCO) due to 2019 novel coronavirus (2019-nCoV) pandemic. Sci. Total Environ. 729 https://doi.org/10.1016/j.scitotenv.2020.139022.

Acker, J.G., Leptoukh, G., 2007. Online analysis enhances use of NASA earth science data Eos. Trans. Am. Geophys. Union 88 (2), 14. https://doi.org/10.1029/2007EO020003.

Adam, M.G., Tran, P.T.M., Balasubramanian, R., 2021. Air quality changes in cities during the COVID-19 lockdown: a critical review. Atmos. Res. 264 https://doi.org/10.1016/j.atmosres.2021.105823. Elsevier Ltd.

Addas, A., Maghrabi, A., 2021. The impact of covid-19 lockdowns on air quality —a global review. Sustainability (Switzerland) 13 (18). https://doi.org/10.3390/su131810212.

Agarwal, N., Meena, C.S., Raj, B.P., Saini, L., Kumar, A., Gopalakrishnan, N., Kumar, A., Balam, N.B., Alam, T., Kapoor, N.R., Aggarwal, V., 2021. Indoor air quality improvement in COVID-19 pandemic: review. Sustain. Cities Soc. 70, 102942. https://doi.org/10.1016/j.scs.2021.102942.

Ahmad, S.P., Levelt, P.F., Bhartia, P.K., Hilsenrath, E., Leppelmeier, G.W., Johnson, J.E., 2003. Atmospheric products from the ozone monitoring instrument (OMI). In: Barnes, W.L. (Ed.), Earth Observing Systems VIII, vol. 5151, p. 619. https://doi.org/10.1117/12.506042.

Aman, M.A., Salman, M.S., Yunus, A.P., 2020. COVID-19 and its impact on environment: improved pollution levels during the lockdown period – a case from Ahmedabad, India. In: Remote Sensing Applications. Society and Environment. https://doi.org/10.1016/j.rsase.2020.100382, 20.

Angom, J., Angiro, C., Omara, T., 2021. Air quality improvement from COVID-19 lockdown in the east african community: evidences from kampala and nairobi cities. OALib 8 (6), 1–26. https://doi.org/10.4236/oalib.1107389.

Badr, O., Probert, S.D., 1994. Sources of Atmospheric Carbon Monoxide.

Barré, J., Petetin, H., Colette, A., Guevara, M., Peuch, V.H., Rouil, L., Engelen, R., Inness, A., Flemming, J., Pérez García-Pando, C., Bowdalo, D., Meleux, F., Geels, C., Christensen, J.H., Gauss, M., Benedictow, A., Tsyro, S., Friese, E., Struzewska, J., et al., 2021. Estimating lockdown-induced European NO2changes using satellite and surface observations and air quality models. Atmos. Chem. Phys. 21 (9), 7373–7394. https://doi.org/10.5194/acp-21-7373-2021.

Barret, T., 2020. Air Quality Making Headlines during the Coronavirus Lockdown.

Behera, M.D., Mudi, S., Shome, P., Das, P.K., Kumar, S., Joshi, A., Rathore, A., Deep, A., Kumar, A., Sanwariya, C., Kumar, N., Chandrakar, R., Seshadri, S., Mukherjee, S., Bhattaram, S.K., Sirivella, Z., 2022. COVID-19 slowdown induced improvement in air quality in India: rapid assessment using Sentinel-5P TROPOMI data. Geocarto Int. 37 (25), 8127–8147. https://doi.org/10.1080/10106049.2021.1993351.

Borge, R., Requia, W.J., Yagüe, C., Jhun, I., Koutrakis, P., 2019. Impact of weather changes on air quality and related mortality in Spain over a 25 year period [1993–2017]. Environ. Int. 133, 105272 https://doi.org/10.1016/j.envint.2019.105272.

Burke, P.J., Best, R., Jotzo, F., 2019. Closures of coal-fired power stations in Australia: local unemployment effects. Aust. J. Agric. Resour. Econ. 63 (1), 142–165. https://doi.org/10.1111/1467-8489.12289.

Chen, B., Kan, H., 2008. Air pollution and population health: a global challenge. Environ. Health Prev. Med. 13 (2), 94–101. https://doi.org/10.1007/s12199-007-0018-5.

Chen, K., Wang, M., Huang, C., Kinney, P.L., Anastas, P.T., 2020. Air pollution reduction and mortality benefit during the COVID-19 outbreak in China. Lancet Planet. Health 4 (Issue 6). https://doi.org/10.1016/S2542-5196(20)30107-8 e210–e212). Elsevier B.V.

Dantas, G., Siciliano, B., França, B.B., da Silva, C.M., Arbilla, G., 2020. The impact of COVID-19 partial lockdown on the air quality of the city of Rio de Janeiro, Brazil. Sci. Total Environ. 729 https://doi.org/10.1016/j.scitotenv.2020.139085.

Ding, F., Iredell, L., Theobald, M., Wei, J., Meyer, D., 2021. PBL height from AIRS, GPS RO, and MERRA-2 products in NASA GES DISC and their 10-year seasonal mean intercomparison. Earth Space Sci. 8 (9) https://doi.org/10.1029/2021EA001859.

Duc, H., Salter, D., Azzi, M., Jiang, N., Warren, L., Watt, S., Riley, M., White, S., Trieu, T., Chang, L.T.C., Barthelemy, X., Fuchs, D., Nguyen, H., 2021. The effect of lockdown period during the covid-19 pandemic on air quality in sydney region, Australia. Int. J. Environ. Res. Publ. Health 18 (7). https://doi.org/10.3390/ijerph18073528.

Eicken, H., Danielsen, F., Sam, J.-M., Fidel, M., Johnson, N., Poulsen, M.K., Lee, O.A., Spellman, K.V., Iversen, L., Pulsifer, P., Enghoff, M., 2021. Connecting top-down and bottom-up approaches in environmental observing. BioScience 71 (5), 467–483. https://doi.org/10.1093/biosci/biab018.

Esmen, N.A., Corn, M., 1971. Residence time of particles in urban air. Atmos. Environ. 5, 571–578.

Fang, C., Yu, D., 2017. Urban agglomeration: an evolving concept of an emerging phenomenon. Landsc. Urban Plann. 162, 126–136. https://doi.org/10.1016/j.landurbplan.2017.02.014.

Feizizadeh, B., Blaschke, T., 2013. Examining urban heat island relations to land use and air pollution: Multiple endmember spectral mixture analysis for thermal remote sensing. IEEE J. Sel. Top. Appl. Earth Obs. Rem. Sens. 6 (3), 1749–1756.

Gardiner, B., 2020. Pollution Made COVID-19 Worse. Now, Lockdowns Are Clearing the Air. https://www.nationalgeographic.com/science/article/pollution-made-the-pandemic-worse-but-lockdowns-clean-the-sky.

Gaur, V.K., Gautam, K., Sharma, P., Gupta, P., Dwivedi, S., Srivastava, J.K., Varjani, S., Ngo, H.H., Kim, S.-H., Chang, J.-S., Bui, X.-T., Taherzadeh, M.J., Parra-Saldívar, R., 2022. Sustainable strategies for combating hydrocarbon pollution: special emphasis on mobil oil bioremediation. Sci. Total Environ. 832, 155083 https://doi.org/10.1016/j.scitotenv.2022.155083.

Gautam, S., 2020. The influence of COVID-19 on air quality in India: a boon or inutile. Bull. Environ. Contam. Toxicol. 104 (6), 724–726. https://doi.org/10.1007/s00128-020-02877-y.

Global Modeling, Assimilation Office (Gmao), 2015. MERRA-2 tavg1_2d_adg_Nx: 2d,1-Hourly,Time-averaged,Single-Level,Assimilation,Aerosol diagnostics (extended) V5.12.4. In: Goddard Earth Sciences Data and Information Services Center. https://doi.org/10.5067/HM00OHQBHKTP *(GES DISC)*.

Holden, Emily, 2020. Trump to Roll Back Obama-Era Clean Car Rules in Huge Blow to Climate Fight. The Guardian. https://www.theguardian.com/environment/2020/mar/31/trump-epa-obama-clean-car-rules-climate-change.

Hsieh, Pi-Fuei, Lee, L.C., Chen, Nai-Yu, 2001. Effect of spatial resolution on classification errors of pure and mixed pixels in remote sensing. IEEE Trans. Geosci. Rem. Sens. 39 (12), 2657–2663. https://doi.org/10.1109/36.975000.

Jephcote, C., Hansell, A.L., Adams, K., Gulliver, J., 2021. Changes in air quality during COVID-19 'lockdown' in the United Kingdom. Environ. Pollut. 272, 116011. https://doi.org/10.1016/j.envpol.2020.116011.

Junkermann, W., Roedel, W., 1983. Evidence for short So2 lifetimes in the atmosphere: an in-situ measurement of atmospheric so2 lifetime using cosmic ray produced Sulfur-38. Atmos. Environ. 17 (12), 2549–2554. https://doi.org/10.1016/0004-6981(83)90082-3, 1967.

Khalil, M.A.K., Rasmussen, R.A., 1990. The global cycle of carbon monoxide: trends and mass balance. Chemosphere 20 (1–2), 227–242. https://doi.org/10.1016/0045-6535(90)90098-E.

Kharroubi, S., Saleh, F., 2020. Are lockdown measures effective against COVID-19? Front. Public Health 8. https://doi.org/10.3389/fpubh.2020.549692.

Kleipool, Q., Rozemeijer, N., van Hoek, M., Leloux, J., Loots, E., Ludewig, A., van der Plas, E., Adrichem, D., Harel, R., Spronk, S., ter Linden, M., Jaross, G., Haffner, D., Veefkind, P., Levelt, P.F., 2022. Ozone Monitoring Instrument (OMI) collection 4: establishing a 17-year-long series of detrended level-1b data. Atmos. Meas. Tech. 15 (11), 3527–3553. https://doi.org/10.5194/amt-15-3527-2022.

Kutralam-Muniasamy, G., Pérez-Guevara, F., Roy, P.D., Elizalde-Martínez, I., Shruti, V. C., 2021. Impacts of the COVID-19 lockdown on air quality and its association with human mortality trends in megapolis Mexico City. Air Quality, Atmos. Health 14 (4), 553–562. https://doi.org/10.1007/s11869-020-00960-1.

Levelt, P.F., Van Den Oord, G.H.J., Dobber, M.R., Mälkki, A., Visser, H., De Vries, J., Stammes, P., Lundell, J.O.V., Saari, H., 2006. The ozone monitoring instrument. IEEE Trans. Geosci. Rem. Sens. 44 (5), 1093–1100. https://doi.org/10.1109/TGRS.2006.872333.

Levelt, P.F., Joiner, J., Tamminen, J., Veefkind, J.P., Bhartia, P.K., Stein Zweers, D.C., Duncan, B.N., Streets, D.G., Eskes, H., van der A, R., McLinden, C., Fioletov, V., Carn, S., de Laat, J., DeLand, M., Marchenko, S., McPeters, R., Ziemke, J., Fu, D., et al., 2018. The ozone monitoring instrument: overview of 14 years in space. Atmos. Chem. Phys. 18 (8), 5699–5745. https://doi.org/10.5194/acp-18-5699-2018.

Li, L., Li, Q., Huang, L., Wang, Q., Zhu, A., Xu, J., Liu, Z., Li, H., Shi, L., Li, R., Azari, M., Wang, Y., Zhang, X., Liu, Z., Zhu, Y., Zhang, K., Xue, S., Ooi, M.C.G., Zhang, D., Chan, A., 2020a. Air quality changes during the COVID-19 lockdown over the Yangtze River Delta Region: an insight into the impact of human activity pattern changes on air pollution variation. Sci. Total Environ. 732 https://doi.org/10.1016/j.scitotenv.2020.139282.

Li, L., Li, Q., Huang, L., Wang, Q., Zhu, A., Xu, J., Liu, Z., Li, H., Shi, L., Li, R., Azari, M., Wang, Y., Zhang, X., Liu, Z., Zhu, Y., Zhang, K., Xue, S., Ooi, M.C.G., Zhang, D., Chan, A., 2020b. Air quality changes during the COVID-19 lockdown over the Yangtze River Delta Region: an insight into the impact of human activity pattern changes on air pollution variation. Sci. Total Environ. 732 https://doi.org/10.1016/j.scitotenv.2020.139282.

Lorente, A., Boersma, K.F., Eskes, H.J., Veefkind, J.P., van Geffen, J.H.G.M., de Zeeuw, M.B., Denier van der Gon, H.A.C., Beirle, S., Krol, M.C., 2019. Quantification of nitrogen oxides emissions from build-up of pollution over Paris with TROPOMI. Sci. Rep. 9 (1), 20033 https://doi.org/10.1038/s41598-019-56428-5.

Manisalidis, I., Stavropoulou, E., Stavropoulos, A., Bezirtzoglou, E., 2020. Environmental and health impacts of air pollution: a review. Front. Public Health 8. https://doi.org/10.3389/fpubh.2020.00014.

Menut, L., Bessagnet, B., Siour, G., Mailler, S., Pennel, R., Cholakian, A., 2020. Impact of lockdown measures to combat Covid-19 on air quality over western Europe. Sci. Total Environ. 741, 140426. https://doi.org/10.1016/j.scitotenv.2020.140426.

Molina, M.J., Molina, L.T., 2004. Megacities and atmospheric pollution. J. Air Waste Manag. Assoc. 54 (6), 644–680. https://doi.org/10.1080/10473289.2004.10470936.

Mukherjee, A., Agrawal, M., 2017. World air particulate matter: sources, distribution and health effects. Environ. Chem. Letts. 15 (2), 283–309. https://doi.org/10.1007/s10311-017-0611-9.

Pearson's correlation coefficient. In: Encyclopedia of Public Health, 2008. Springer Netherlands, pp. 1090–1091. https://doi.org/10.1007/978-1-4020-5614-7_2569.

Popescu, F., Ionel, I., 2010. Anthropogenic air pollution sources. In: *Air Quality*. Sciyo. https://doi.org/10.5772/9751.

Rana, R.H., Keramat, S.A., Gow, J., 2021. A systematic literature review of the impact of COVID-19 lockdowns on air quality in China. In: Aerosol and Air Quality Research, vol. 21. https://doi.org/10.4209/aaqr.200614. Issue 8). AAGR Aerosol and Air Quality Research.

Ravindra, K., Sokhi, R., Van Grieken, R., 2008. Atmospheric polycyclic aromatic hydrocarbons: source attribution, emission factors and regulation. Atmos. Environ. 42 (13), 2895–2921. https://doi.org/10.1016/j.atmosenv.2007.12.010.

Ravindra, K., Singh, T., Vardhan, S., Shrivastava, A., Singh, S., Kumar, P., Mor, S., 2022. COVID-19 pandemic: what can we learn for better air quality and human health? J. Infect. Public Health 15 (2), 187–198. https://doi.org/10.1016/j.jiph.2021.12.001.

Rodríguez-Urrego, D., Rodríguez-Urrego, L., 2020. Air quality during the COVID-19: PM2.5 analysis in the 50 most polluted capital cities in the world. Environ. Pollut. 266, 115042. https://doi.org/10.1016/j.envpol.2020.115042.

Schiavo, B., Morton-Bermea, O., Arredondo-Palacios, T.E., Meza-Figueroa, D., Robles-Morua, A., García-Martínez, R., Valera-Fernández, D., Inguaggiato, C., Gonzalez-Grijalva, B., 2022. Analysis of COVID-19 lockdown effects on urban air quality: a case study of monterrey, Mexico. Sustainability 15 (1), 642. https://doi.org/10.3390/su15010642.

Schiermeier, Q., 2020. Why pollution is falling in some cities — but not others. Nature 580, 313.

Shepherd, M., Andersen, T., Strother, C., Horst, A., Bounoua, L., Mitra, C., 2013. Urban climate archipelagos: a new framework for urban impacts on climate. Earthzine 1–10. http://www.earthzine.org/2013/11/29/urban-climate-archipelagos-a-new-framework-for-urban-impacts-on-climate/.

Smith, S.J., Van Aardenne, J., Klimont, Z., Andres, R.J., Volke, A., Delgado Arias, S., 2011. Anthropogenic sulfur dioxide emissions: 1850-2005. Atmos. Chem. Phys. 11 (3), 1101–1116. https://doi.org/10.5194/acp-11-1101-2011.

Spiegel, M., Tookes, H., 2022. All or nothing? Partial business shutdowns and COVID-19 fatality growth. PLOS ONE 17 (2), e0262925. https://doi.org/10.1371/journal.pone.0262925.

The Royal Society, 2008. Ground-level Ozone in the 21st Century: Future Trends, Impacts and Policy Implications Science Policy.

Tian, H., Xu, R., Canadell, J.G., Thompson, R.L., Winiwarter, W., Suntharalingam, P., Davidson, E.A., Ciais, P., Jackson, R.B., Janssens-Maenhout, G., Prather, M.J., Regnier, P., Pan, N., Pan, S., Peters, G.P., Shi, H., Tubiello, F.N., Zaehle, S., Zhou, F., et al., 2020. A comprehensive quantification of global nitrous oxide sources and sinks. Nature 586 (7828), 248–256. https://doi.org/10.1038/s41586-020-2780-0.

TOMS Science Team, 1996. TOMS Meteor-3 Total Ozone UV-Reflectivity Daily L3 Global 1 Deg X 1.25 Deg V008. Goddard Earth Sciences Data and Information Services Center (GES DISC). https://disc.gsfc.nasa.gov/datacollection/TOMSM3L3_008.html.

Wang, Y., Yuan, Y., Wang, Q., Liu, C.G., Zhi, Q., Cao, J., 2020. Changes in air quality related to the control of coronavirus in China: implications for traffic and industrial emissions. Sci. Total Environ. 731, 139133 https://doi.org/10.1016/j.scitotenv.2020.139133, 2019.

Wang, T., Xue, L., Feng, Z., Dai, J., Zhang, Y., Tan, Y., 2022. Ground-level ozone pollution in China: a synthesis of recent findings on influencing factors and impacts. In Environmental Research Letters. Inst. Phys. 17 (6) https://doi.org/10.1088/1748-9326/ac69fe.